Title
Circadian deficits and therapies in mouse models of Huntington's disease

Author
Truong, Danny

Publication Date
2014

Peer reviewed|Thesis/dissertation

UNIVERSITY OF CALIFORNIA

Los Angeles

Circadian deficits and therapies in mouse models of Huntington's disease

A thesis submitted in partial satisfaction

of the requirements for the degree

Master of Science in Integrative Biology and Physiology

by

Danny Truong

2014

ABSTRACT OF THE THESIS

Circadian deficits and therapies in mouse models of Huntington's disease

Master of Science in Integrative Biology and Physiology

University of California, Los Angeles, 2014

Professor Christopher S. Colwell, Co-Chair

Professor Gene Block, Co-Chair

by

Danny Truong

Huntington's disease (HD) is an autosomal dominant neurodegenerative disease caused by a CAG repeat expansion in the *huntingtin* gene. Patients report cognitive and psychiatric difficulties as well as disruptions in their sleep/wake cycles prior to the onset of the motor symptoms. I assessed three HD mouse models (transgenic BACHD, Q175 knock-in, and 3-NP mitochondrial toxin treatment) and show that each model exhibited sleep and circadian deficits. Next, I sought to stabilize and rescue the circadian rhythms of the BACHD mouse model by keeping the mice on a regular feeding schedule. Measurements of cognition, motor coordination, sleep and circadian rhythms were taken before and after a 3-month treatment. My results indicate that scheduled feeding can improve circadian, sleep, and cognitive performance. While motor performance did not improve, the tests showed no further decline during treatment. Thus, the experimental data supports the use of temporally restricting feeding as a lifestyle-based therapeutic.

The thesis of Danny Truong is approved.

Christopher S. Colwell, co-chair

Gene Block, co-chair

Fernando Gomez-Pinilla

University of California, Los Angeles

2014

Table of Contents

List of Figures

Acknowledgements

I would like to thank all the members of the Colwell Lab for years of support and encouragement. Firstly, an appreciation to my committee, Gene Block, Fernando Gomez-Pinilla, and Christopher Colwell, for advising me throughout the Master's program. In particular, I would like to thank Christopher Colwell for giving me the opportunity and privilege of working in his lab beginning as an undergraduate volunteer washing mice cages. Much gratitude also for Dawn Loh for her guidance and patience in working with me all these years, helping me hone my skills to become a better researcher. The rest of the lab have also been supportive in allowing me to work on their projects or have assisted me in numerous experiments: Takashi Kudo, Analyne Schroeder, Andy Vosko, Dika Kuljis, Quan Li, Yingfei Wu, Richard Flores, Matthew Derakhshesh, Laura Gad, Jingyi Qian, Zoë A. MacDowell Kaswan, Olivia Hitchcock, Rishika Singh, Tara Hallman, and many others I'm sure I've missed. I truly value everyone's friendships and the camaraderie we've developed over the years working together in the lab.

Friends in the Masters program, friends at Grace Community Church, and especially my family have also been pivotal in helping me endure through the trials and joys in life while in graduate school, and for keeping me grounded and putting everything in perspective. I am thankful for the blessing you've all been in my life, giving it indescribable vibrancy and depth.

Finally, I would like to acknowledge the CHDI Foundation (http://chdifoundation.org/) for funding the research.

Chapter 1

Circadian deficits in the mouse models of Huntington's disease

Introduction

Circadian rhythms regulate physiological functions in an organism with an endogenous clock that cycles approximately every 24 hours(Dibner, Schibler, & Albrecht, 2010). At the molecular level, these rhythms are driven by a transcription-translation feedback loop. In order to adapt to changing environmental conditions, mammals have a specialized light detection system located in the retina capable of non-visual light detection through melanopsin containing retinal ganglion cells. Light information is carried from the retina, through the retinohypothalamic tract, to the suprachiasmatic nucleus (SCN) of the hypothalamus. The SCN acts as the master pacemaker in mammals, integrating the incoming light information and signaling downstream through a variety of outputs such as neural and hormonal signals. These signals to the rest of the body synchronize peripheral oscillators such as molecular clocks in the heart, liver, and adrenals.

Disruption of these circadian rhythms can negatively impact health. Misalignment of these rhythms increase the risk of metabolic and cardiovascular disease(Scheer, Hilton, Mantzoros, & Shea, 2009), cognitive deficits(Loh et al., 2010), and psychiatric disorders(Mcclung, 2011). Patients with Huntington's disease suffer from sleep/wake disturbances, suggesting deficits in their circadian rhythms(Morton et al., 2005; Wiegand, Möller, Schreiber, Lauer, & Krieg, 1991). Huntington's disease (HD) is an autosomal dominant neurodegenerative disease, caused by an expansion of the CAG repeats in the *huntingtin* gene(Kudo et al., 2011; Maywood et al., 2010; The Huntington's Disease Collaborative Research Group, 1993). Longer repeats positively correlates with an earlier disease onset. While most commonly associated with involuntary movements (Huntington's chorea), patients suffer from a variety of symptoms even prior to the onset of the motor symptoms: trouble falling asleep and excessive daytime sleepiness, cognitive decline, and psychiatric disorders(Marshall et al., 2007; Stout et al., 2011). The same symptoms parallel ones seen with disrupted circadian

rhythms, suggesting that treating their circadian rhythms can improve their quality of life for both the patients and their caretakers(Goodman & Barker, 2010; Morton et al., 2005).

A number of mouse models for Huntington's disease have been generated over the years. One of the models is the bacterial artificial chromosome (BAC)-mediated transgenic mouse (BACHD) (Gray et al., 2008). Another model is the Q175 line of mice, with a spontaneous expansion of the CAG repeats in the CAG140 KI line(Menalled et al., 2012). Finally, a third model is the treatment with mitochondrial complex II toxin, 3-nitropropionic acid (3-NP), widely used to study the striatal pathology seen in HD(Brouillet, 2014). The purpose of the initial studies was to assess whether the three mouse models (BACHD, Q175, and 3-NP) recapitulate the symptoms seen in Huntington's disease patients. I assessed the circadian phenotype of these three mouse models by monitoring their running wheel activity and sleep patterning, along with characterization of the motor deficits in the Q175 line of mice.

Methods

Mouse models

The experimental protocols used in this study were approved by the UCLA Animal Research Committee (ARC 2009-022), and all recommendations for animal use and welfare, as dictated by the UCLA Division of Laboratory Animal Medicine and the guidelines from the National Institutes of Health, were followed.

The BACHD mice are on the C57BL6/J background(Gray et al., 2008). Mutants and littermate wild-type (WT) controls were obtained from the mouse mutant resource at JAX (The Jackson Laboratory, Bar Harbor, Maine) in a colony maintained by the CHDI Foundation. For each line, we studied littermate mutants and WT controls in parallel.

The Q175 line of mice was obtained from the CHDI colony at JAX, derived from a spontaneous expansion of the CAG repeats in the CAG140 KI line. The Q175 mice have previously been shown to have around 188 CAG repeats(Menalled et al., 2012). We obtained an age-matched cohort of male mice on the C57Bl6/J background that were wild-type (WT), heterozygote (Het) and homozygote (Hom) for the Q175 allele.

The third group of mice consisted of C57BL/6 mice from breeding colonies at UCLA with intraperitoneal (i.p., 15 mg/kg) injections of a Complex II inhibitor, 3-nitropropionic acid, 3-NP (Sigma–Aldrich) dissolved in phosphate buffer (pH7.4). Control mice were administered with saline at a dose of 10 ml/kg. The mice were injected for 5 consecutive days, with injections at Zeitgeber time (ZT) 9 (9 h after lights on).

Running wheel cage activity

Mice were singly housed in cages containing wheels (11.5 cm diameter, Mini Mitter, Bend, OR), and locomotor activity was recorded as previously described(Colwell et al., 2003). They were entrained to a 12:12 hour light:dark (LD) cycle for a minimum of 2 weeks prior to collection of 10–

14 days of data under LD conditions, followed by 10–14 days in constant darkness (DD) to obtain free-running activity. The behavioral response to a phase delaying 10 min pulse of light (100 lux at cage level) at circadian time (CT) 16 was measured as previously described(Colwell et al., 2003). Following these assays, the mice were entrained to 12:12 LD for a minimum of 14 days.

Wheel revolutions were recorded in 3 min bins, and 10 days of data under each condition were averaged for analysis. Free-running period (tau, τ) was determined using the χ^2 periodogram(Sokolove & Bushell, 1978) and the power of the rhythm was determined by multiplying the amplitude, Qp, by 100/n, where n=number of datapoints examined using the El Temps program (A. Diez-Noguera, Barcelona, Spain). Activity amount was determined by averaging 10 days of wheel revolutions (rev/hr). Activity duration (alpha, α) was determined by the duration of activity over the threshold of the mean using an average waveform of 10 days of activity. Nocturnality was determined from the average percentage of activity conducted during the dark. Precision was determined by calculating the daily variation in onset from a best-fit regression line drawn through 10 days of activity in both LD and DD conditions using the ClockLab program (Actimetrics, Wilmette, IL). Fragmentation was defined by bouts/day, where each bout was counted when activity was separated by a gap of 21 minutes or more (maxgap setting of 21 min).

The BACHD (WT *n*=8, BACHD *n*=8) and Q175 (WT *n*=8, Q175 Het *n*=8, Q175 Hom *n*=8) mice were continuously housed in the same environment and subjected to the same battery of lighting conditions and assays at each age mark (3, 6, 9, and 12 months). Only the Q175 mice were removed from these conditions to record motor function (at 6, 9 and 12 months as described below) and behavioral sleep (at 9 and 12 months). BACHD mice had sleep assessed at 3 and 12 months. 3NP mice (WT *n*=8, 3NP *n*=8) had their cage activity and sleep assessed at 2 months of age.

Immobility defined sleep

Manual scoring

BACHD mutants and their WT littermates were first entrained to a 12:12 LD cycle for at least 2 weeks. The mice were housed individually in the absence of wheels and recorded using a video surveillance camera system (Gadspot Inc., City of Industry, CA). The sleep state is marked by several easily observed behaviors, including adoption of a species-specific sleep posture with the eyes closed(Campbell & Tobler, 1984). A mouse was scored as being asleep only when its eyes were closed as it lay on its side, or if it was curled up with its head tucked into its body, or if the mouse did not make any movements other than brief transitional changes in posture for durations of at least 40s. Others have previously employed this method to determine the basic temporal distribution of behavioral sleep across a 24-h period(Loh et al., 2010; Pack et al., 2007). Sleep/wake behavior was scored visually in 5 min intervals, which were summed and averaged to determine day and night percentages of time spent in sleep. Consolidation was determined by counting the number of consecutive bins of sleep that exceeded 20 min in duration.

Automated scoring

Q175 (WT, Het, and Hom) and 3NP mice were habituated to see-through plastic cages containing bedding, but without the addition of nesting material, for a minimum of 3 days prior to video recording of behavior. A side-on view of each cage was obtained, with minimal occlusion by the food bin or water bottle, both of which were top-mounted. Video capture was accomplished using surveillance cameras with visible light filters (Gadspot Inc., City of Industry, CA) connected to the video- capture card (Adlink Technology Inc., Irvine, CA) on a Dell Optiplex computer system. The ANY-maze software (Stoelting Co., Wood Dale, IL) was used to track the animals as described by Fisher and colleagues(Fisher et al., 2012), who found 99% correlation between immobility-defined and EEG-defined sleep using an immobility detection threshold set to 95% of the area of

the animal immobile for 40 seconds. Immobility-defined sleep in this study is thus defined as 95% immobility recorded in an animal for a minimum of 40 seconds.

Continuous recording and tracking of the mice under a 12:12 LD cycle was performed for a minimum of 3 days, with randomized visits (1/day) by the experimenter to confirm mouse health and video recording. We used data collected from days 2 and 3 for further analysis. Immobility-defined sleep data were exported in 1 min bins, and total sleep was determined by summing the duration of sleep in the day (ZT 0–12) or night (ZT 12–24). Number of sleep bouts was determined using ClockLab at the resolution of 1 min bins of ANY-maze data (minimum of 40 sec sleep per bin). Average bout duration (number of consecutive bins with at least 40 sec of sleep per bin) was determined within day or night. An average waveform of hourly sleep from both days was produced per genotype per age group for the purpose of graphical display.

Motor tests

On only the Q175 mice, we employed both the accelerating rotarod test(Menalled et al., 2009) and challenging beam test(Fleming, Salcedo, & Fernagut, 2004) to determine the progression of motor dysfunction in the mice. All tests were performed at the light:dark transition (ZT 11 to 12; one hour prior to lights-off) to minimize effects of sleep deprivation.

At 6, 9 and 12 months, the mice were trained on the rotarod (Ugo Basile, Varese, Italy) with 5 trials on the first day, as previously described(Menalled et al., 2009). The accelerating rotarod went from 5 to a maximum of 38 rpm and the maximum length of each trial was 600 sec. On the second day, mice were placed on the rotarod and the latency to fall from the rotarod was recorded from 5 trials, and averaged between trials.

We employed a modified version of the traditional beam walking test, as described in detail by Fleming and colleagues(Fleming et al., 2004). The premise of this task, named the challenging beam test, is to determine the ability of mice to cross a bridge of decreasing width, with re-entry into

the home cage as the motivating factor(Fleming et al., 2004). The beam narrows in 4 intervals from 33 mm > 24 mm > 18 mm > 6 mm, with each bridge spanning 253 mm in length. Mice at 9 and 12 months of age were trained on the beam for 5 consecutive trials at ZT 11 on two consecutive days. During each trial, each mouse was placed on the widest end of the beam and allowed to cross with minimal handling by the experimenter. On the third day, the mice were further challenged during testing by the application of a metal grid (10 X 10 mm spacing) overlaid onto the bridge. A second experimenter was on hand to record the progress of the animal using a hand held camcorder and five consecutive trials were recorded. The videos were scored by two independent observers blind to the experimental conditions for the time to cross the beam and touch the home cage, the number of steps taken by the left hind limb, and the number of missteps (errors) made by each mouse. We considered an error to have occurred when more than half of the foot in question dipped below the grid. Time to cross, number of steps, and number of errors were averaged across the 5 trials per mouse to give the final reported values.

Statistical methods

The BACHD running wheel activity data sets were analyzed by a two-way analysis of variance (ANOVA) comparing factors of age and genotype. If significant group differences were detected ($P < 0.05$) by the ANOVA, then the post-hoc analysis was applied. If the data passed an equal variance test, Tukey's method was applied and if the data failed an equal variance test, Holm–Sidak method was applied. For all tests, alpha was set at $P < 0.05$.

For comparison of WT, Q175 Het, and Hom locomotor activity and sleep parameters that passed normality and equal variance tests within each age group, we applied one way analysis of variance (ANOVA) for which we report the F statistic, and deemed differences as significant if $P < 0.05$. For any parameter that failed either normality or equal variance tests, ANOVA on ranks was applied and H values reported. To compare the effects of gene dosage and age, we applied two way

repeated measures ANOVA. Post hoc Bonferroni's t-test pairwise comparisons were applied in the event of significant effects of genotype or age. In the instance of failed normality or equality, Dunn's method was used instead. Values are reported as mean ± standard error of the mean (SEM). All tests were performed using SigmaStat (version 3.5, SYSTAT Software, San Jose, CA).

Results

BACHD

Diurnal and circadian rhythms of running wheel activity is disrupted in the BACHD model of HD

I used running wheel activity to determine the impact of the mutations on diurnal and circadian rhythms of behavior. The locomotor activity in the BACHD compared to the WT littermates at 3, 6, 9, and 12 months of age showed low amplitude, fragmented rhythms, and a long free-running period. In particular, the BACHD mice had a bimodal activity pattern. There is a progressive decline in their amplitude of rhythms as they age (figure 1, table 1). For example, a two-way ANOVA for age and genotype of their activity in DD revealed an effect of age ($F_{3,40}$ = 3.48, P = 0.02) and genotype ($F_{1,40}$= 43.38, $P < 0.001$). A post-hoc Tukey's test indicates an effect of the BACHD mutation in all age groups. By three months of age, the BACHD show disrupted daily and circadian rhythms in running wheel activity.

WT, as nocturnal animals, have most of their running wheel activity during the night (93% of total activity). On the other hand, the BACHD had a significant amount of activity in the light (24%; t_{14} = -3.54, $P < 0.001$). Deficits in their light-response may explain this phenotype. To test this hypothesis, WT littermates were exposed to white light at CT 16 (100 lx, 10 min duration), showing a 113 ± 5 min (n = 8) phase delay. The BACHD mice had a 55% reduction in magnitude of phase delay after the same light treatment (51 ± 10 min, n = 8; t_{15} = 5.53, P < 0.01). This suggests a deficit in the light response of the circadian system, particularly the phase shifting effect.

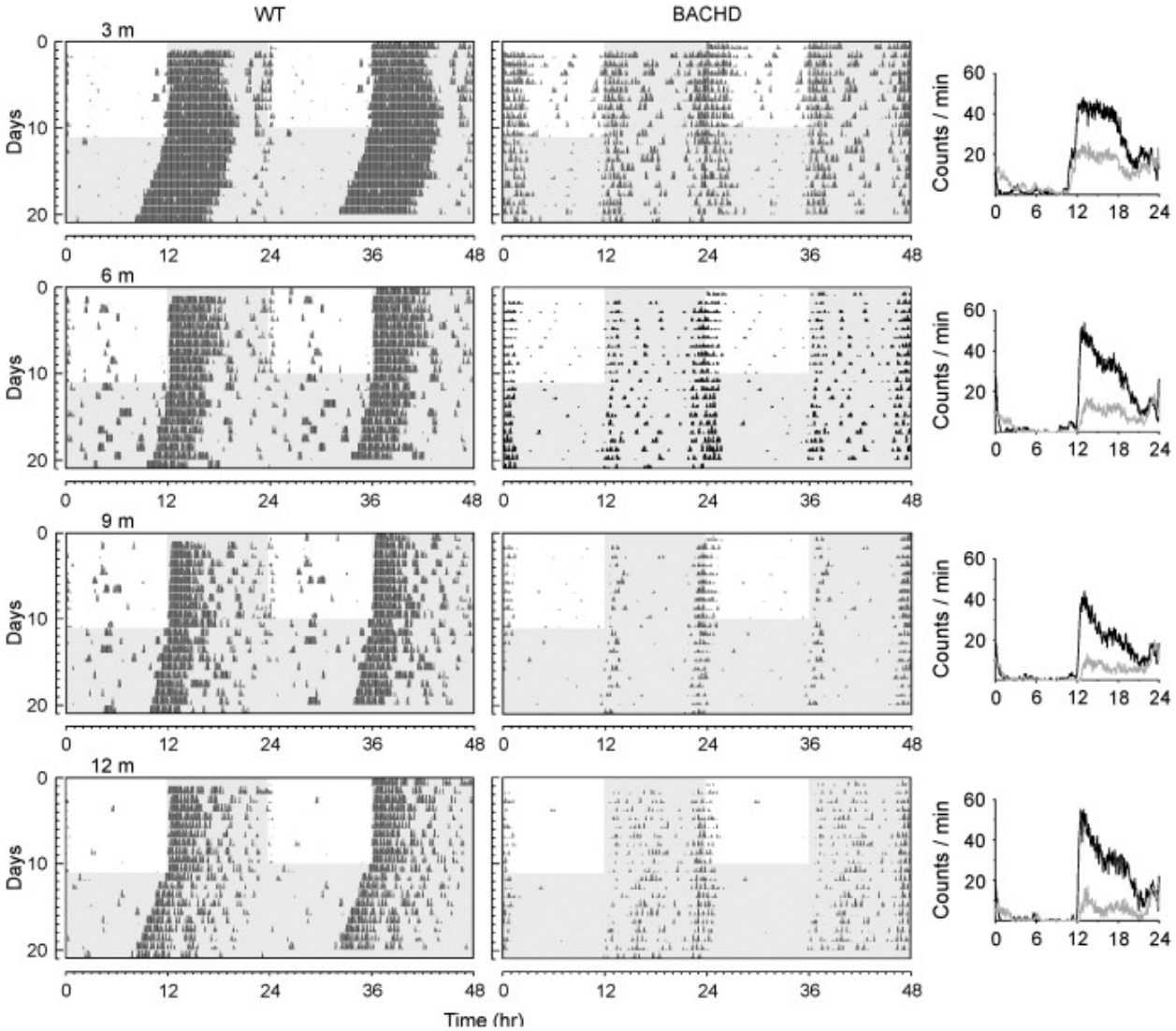

Figure 1: BACHD mice show an age-related decline in activity levels.
Representative actograms from WT animals (left panel) and BACHD littermates (middle panels) at 3, 6, 9, and 12 months of age. The average waveform of activity for each genotype (black line = WT; gray line = BACHD) is shown (right panel). Reprinted with permission from (Kudo et al., 2011)

Genotype	WT	BACHD
LD		
Power (% variation)		
3 mo	59.5 ± 2.7	34.5 ± 3.7*
6 mo	55.1 ± 3.3	42.4 ± 2.9*
9 mo	54.3 ± 3.3	32.9 ± 3.6*
12 mo	55.0 ± 2.0	32.8 ± 3.5*
Activity (rev/h)		
3 mo	981 ± 70	628 ± 99*
6 mo	713 ± 73	297 ± 52*#
9 mo	760 ± 127	277 ± 47*#
12 mo	734 ± 118	233 ± 58*#
DD		
Tau (hrs)		
3 mo	23.69 ± 0.05	24.07 ± 0.04*
6 mo	23.61 ± 0.12	24.05 ± 0.04*
9 mo	23.54 ± 0.08	24.12 ± 0.06*
12 mo	23.69 ± 0.06	23.96 ± 0.02*
Power (% variation)		
3 mo	50.8 ± 5.5	31.0 ± 4.3*
6 mo	51.2 ± 4.8	34.7 ± 2.9*
9 mo	45.8 ± 3.8	31.2 ± 2.1*
12 mo	45.1 ± 2.4	27.5 ± 2.3*
Activity (rev/hr)		
3 mo	1050 ± 34	543 ± 121*
6 mo	872 ± 149	265 ± 50*
9 mo	749 ± 165	229 ± 49*
12 mo	762 ± 98	190 ± 19*#
Fragmentation (bouts/day)		
3 mo	4.4 ± 0.4	7.4 ± 0.8*
6 mo	4.5 ± 0.9	7.3 ± 0.8*
9 mo	5.1 ± 0.6	7.2 ± 0.8*
12 mo	5.0 ± 0.2	8.1 ± 0.4*
Bimodal (%)		
3 mo	0%	37.5%
6 mo	0%	62.5%
9 mo	0%	66.7%
12 mo	0%	50%

Table 1: Age-related decline in amplitude of wheel-running activity rhythms in BACHD mice.
Comparisons between age and genotype were made between littermate WT and mutant mice with a 2-way ANOVA followed by Tukey's post hoc analysis with * indicating a significant difference at $P < 0.05$ between genotypes within age and # indicating $P < 0.05$ between ages within genotype. Reprinted with permission from (Kudo et al., 2011)

Temporal distribution of sleep is altered in the BACHD model

To study the sleep patterning of the BACHD mice, we measured immobility-defined sleep in the young adult (3m) and middle age (12m) BACHD and WT littermates. Both genotypes showed more daytime sleep at 12m than at 3m (two way ANOVA $F_{1,29} = 18.44$, $P < 0.001$). The post-hoc Tukey's t-test revealed that the BACHD mutants had significantly less daytime sleep than WT at 3

months of age (t_{20} = 2.07, P = 0.049). A more detailed analysis revealed that the BACHD mutants had less sleep than the WT littermates at the early day (figure 2, two way repeated measures ANOVA, $F_{7,20}$ = 2.82, P = 0.009). Post-hoc analysis by Tukey's t-tests revealed that the BACHD mutants spent significantly less time in sleep during the hours of ZT 0 - 3 (t_{20} =2.99, P = 0.003) and ZT 3 - 6 (t_{20} = 2.36, P = 0.02).

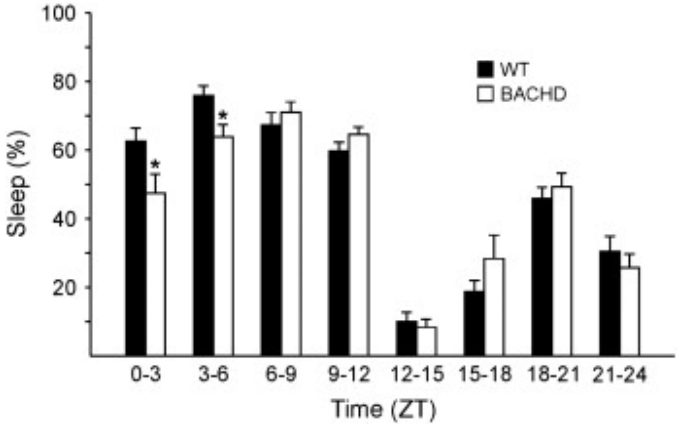

Figure 2: Sleep patterning of WT and BACHD littermates at 3 months of age.
BACHD mice showed significantly reduced sleep during early day. * indicates a difference between BACHD and WT with P < 0.05. Reprinted with permission from (Kudo et al., 2011)

Q175

Q175 mutant mice show age and gene dosage-related decline in circadian rhythms of wheel running activity

An age-matched cohort of WT, Q175 Het, and Q175 Hom mice were assessed using in-cage running wheels to assess their circadian locomotor activity. While young adult Q175 mutants (3 and 6m) were not significantly different from WT, the strength of rhythms (power) declined in the Q175 Hom mice between the 6 and 9-month time point (figure 3, 4). Specifically, this decline is characterized by the decrease in power of rhythms (figure 6B, 7B), precision (figure 6C, 7C), and amount of activity in LD and DD conditions (figure 6D, 7D). At 12 months, the circadian deficits progressed further in the Q175 Hom mice lower nocturnality, power of rhythms, precision, and total activity under LD and DD. The Q175 Het mutants also show an age-related decline in the power of

activity in LD but to a lesser degree compared to the Q175 Hom mutants, indicating an effect of gene dosage.

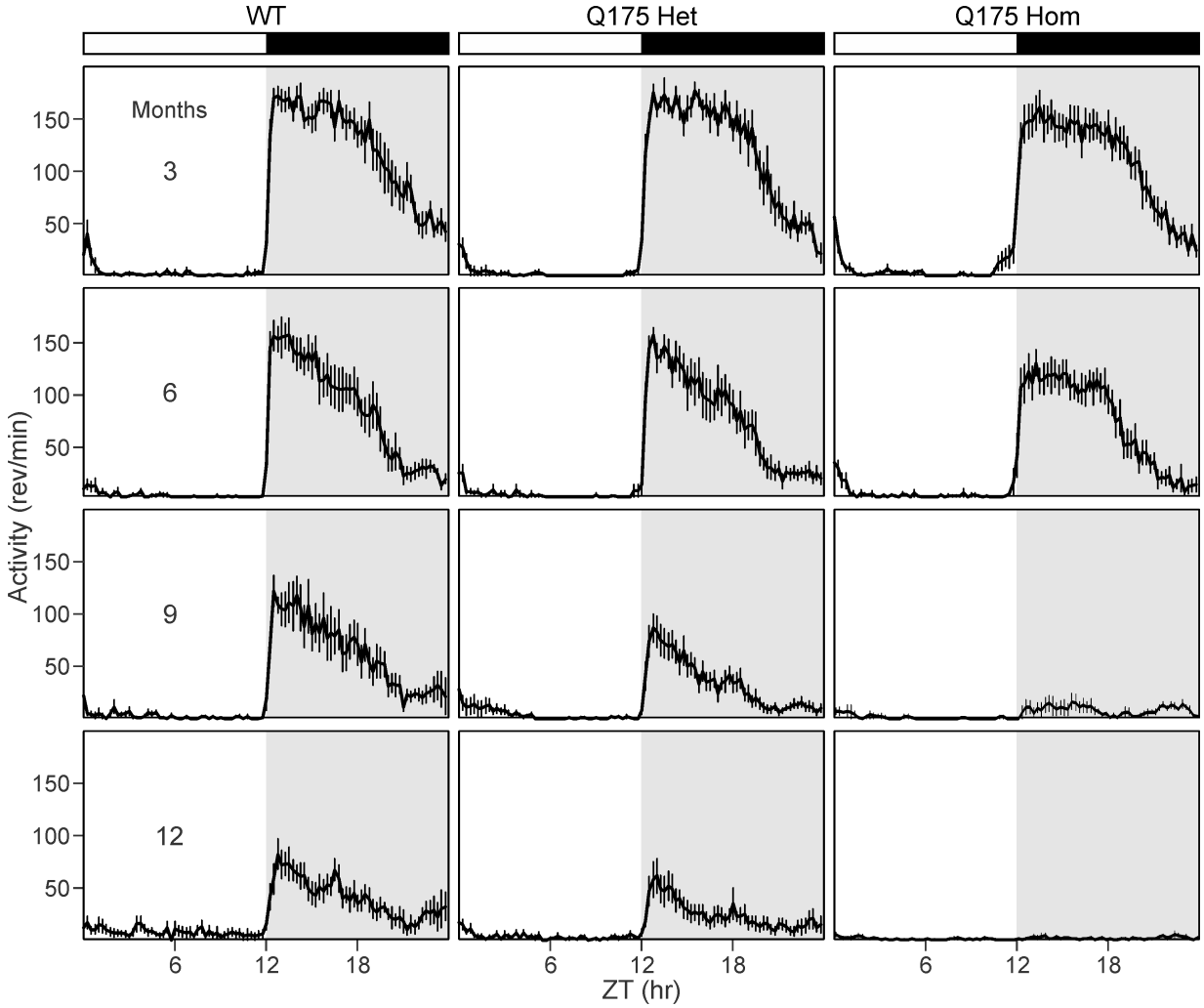

Figure 3: Representative waveforms of running wheel activity at 3, 6, 9, and 12 months of age.
Average waveforms from 10 days of activity in LD. White/black bar at the top indicates 12:12 light:dark cycles. Left to right: WT, Q175 Het, Q175 Hom. Top to bottom: 3, 6, 9, and 12 months of age. Reprinted under Creative Commons Attribution License from (Loh, Kudo, Truong, Wu, & Colwell, 2013)

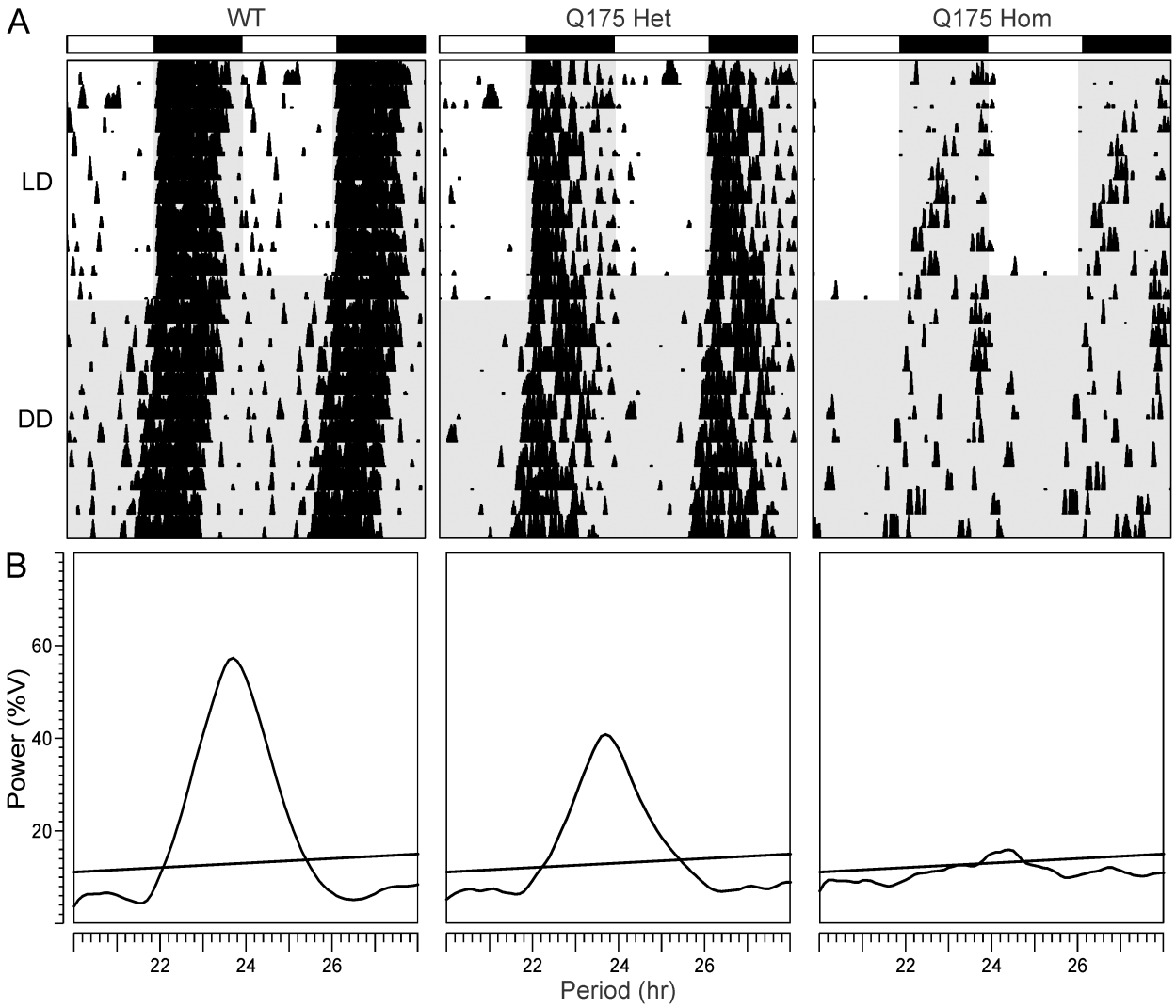

Figure 4: Circadian deficits in the Q175 mice at 9 months of age.
A. Representative double plotted actograms of running wheel activity from WT (left), Q175 Het (middle) and Q175 Hom (right) mice under 10 days of 12:12 light:dark (LD) and 10 days of constant darkness. White/black bars indicate the LD cycle, and the gray shading indicates darkness. Successive days are plotted from top to bottom.
B. Chi-square periodograms of 10 days of activity in DD for the three genotypes at 9 months of age. Peak of periodogram indicates the free-running period of each mouse. Power (%V) refers to the normalized amplitude of the periodogram. Diagonal line indicates significance to $P < 0.05$.
Reprinted under Creative Commons Attribution License from (Loh et al., 2013)

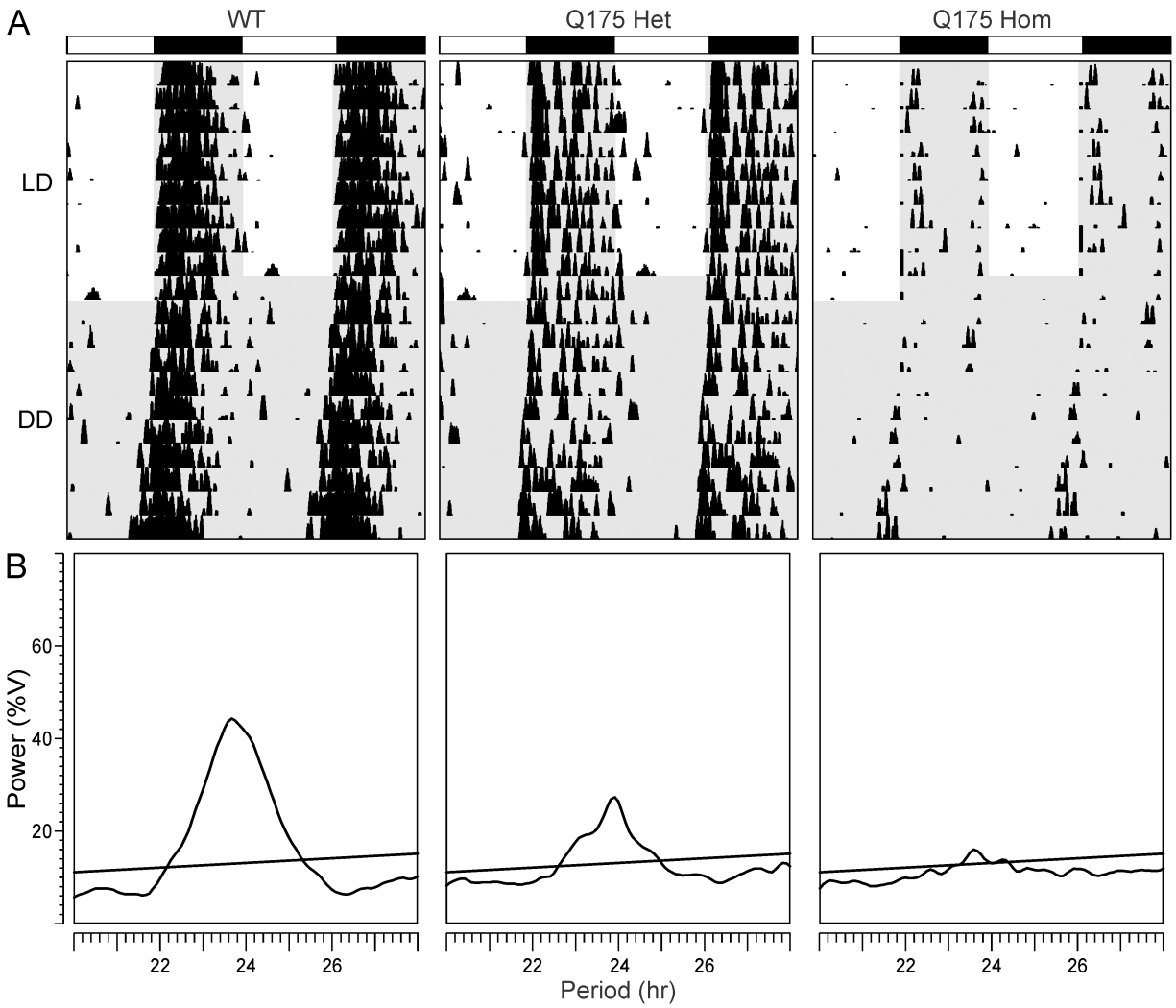

Figure 5: Circadian deficits in locomotor activity in Q175 mutant mice at 12 months of age.
A. Representative double plotted actograms of running wheel activity from WT (left), Q175 Het (middle) and Q175 Hom (right) mice under 10 days of 12:12 light:dark (LD) and 10 days of constant darkness. White/black bars indicate the LD cycle, and the gray shading indicates darkness. Successive days are plotted from top to bottom.
B. Chi-square periodograms of 10 days of activity in DD for the three genotypes at 12 months of age. Peak of periodogram indicates the free-running period of each mouse. Power (%V) refers to the normalized amplitude of the periodogram. Diagonal line indicates significance to $P < 0.05$.

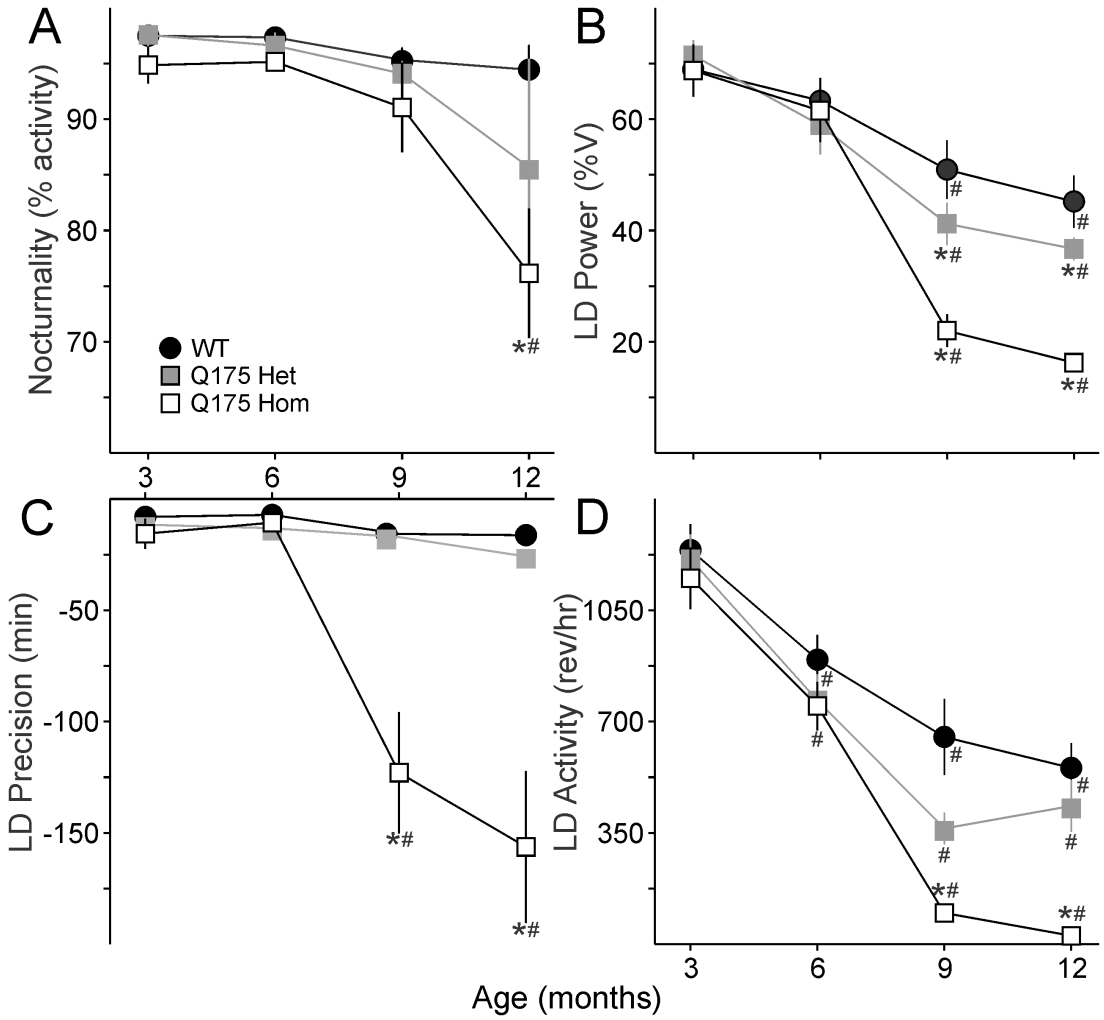

Figure 6: Gene-dosage and age-related decline in rhythms of locomotor activity in Q175 mutants in LD conditions.

A. The percentage of activity at night (nocturnality) declines at 12 months in Q175 Hom mutants.

B. Power (%V), as measured by the χ^2 periodogram, declines dramatically in Q175 Het and Q175 Hom mutants beginning at 9 months.

C. The cycle-to-cycle activity onset is less precise in Q175 Hom mutants from 9 months.

D. The amount of activity (wheel revolutions per hour, rev/hr) declines sharply in Q175 Hom mutants at 9 months.

* indicates significance to $P < 0.05$ in post-hoc pairwise comparisons with WT within each age group after the two way ANOVA revealed an effect of genotype. # indicates an effect of age within each genotype. Reprinted under Creative Commons Attribution License from (Loh et al., 2013)

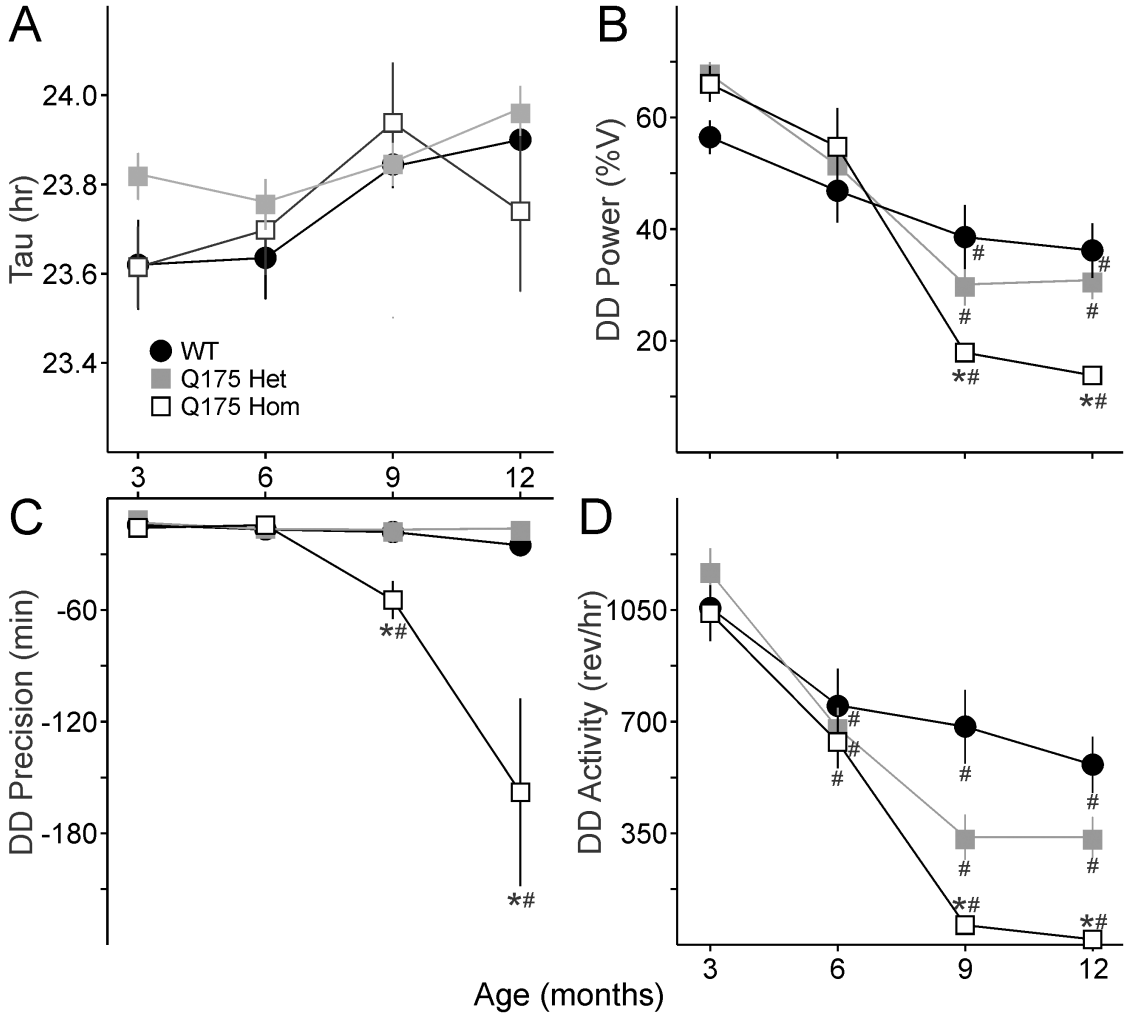

Figure 7: Gene-dosage and age-related decline in rhythms of locomotor activity in Q175 mutants in DD conditions.

A. Free-running period (tau) is not significantly different between the three genotypes.

B. Power, as measured by the χ^2 periodogram, declines in Q175 Hom mutants beginning at 9 months.

C. The cycle-to-cycle activity onset is less precise in Q175 Hom mutants from 9 months.

D. The amount of activity (wheel revolutions per hour, rev/hr) declines in Q175 Hom mutants at 9 months.

* indicates significance to $P < 0.05$ in post-hoc pairwise comparisons with WT within each age group after the two way ANOVA revealed an effect of genotype. # indicates an effect of age within each genotype. Reprinted under Creative Commons Attribution License from (Loh et al., 2013)

Gene-dosage and age-related decline of motor function in Q175 mutant mice

To assess whether the mice showed deficits in motor ability, two motor tests were performed: the accelerating rotarod test and the challenge beam test. At 6 months of age, the

rotarod test showed no effect of genotype on motor function as measured by the latency to fall from rotarod ($F_{2,22} = 0.88$, $P = 0.430$). At 9 months, the Q175 Het and Hom surprisingly showed better performance on the test compared to WT ($F_{2,22} = 2.935$, $P = 0.076$). At 12 months, the test showed a gene dose-related decline in motor function (figure 8a, $F_{2,22}=11.557$, $P < 0.001$). Post-hoc comparisons reveal that Het mice performed worse than WT ($t = 2.419$, $P = 0.025$) and Hom mice performed worse than both age-matched Het and WT mice (vs. Het $t = 2.225$, $P = 0.0378$; vs. WT $t = 4.806$, $P = 0.017$).

The challenge beam test was performed at 9 and 12 months of age. The Q175 Hom mice had difficulty crossing the beam, with longer time to cross the beam at 9 and 12m (figure 8b; 9 months $F_{2,22} = 3.85$, $P = 0.039$; 12 months $F_{2,18} = 6.91$, $P = 0.007$) and greater number of errors compared to WT and Q175 Het (figure 8C; 9 months $F_{2,22} = 13.569$, $P < 0.001$; 12 months $F_{2,18} = 17.794$, $P < 0.001$). At 12m, 4 of 8 of the Hom were unable to cross the mean and excluded from analysis. The deterioration in challenging beam performance with age was tested using two way ANOVA, which did not reveal a significant effect of age on the time to cross the challenging beam (age $F_{1,41} = 3.341$, $P = 0.076$; genotype $F_{2,41} = 10.761$, $P < 0.001$). On the other hand, the number of errors made while crossing the beam was both age- and genotype-dependent (age $F_{1,41} = 31.575$, $P < 0.001$; genotype $F_{2,41} = 32.741$, $P < 0.001$). As compared to the WT mice, the Q175 Hom mice showed deficits in the challenge beam test beginning at 9 months, and Q175 Het and Hom mice showed deficits in the rotarod test at 12 months.

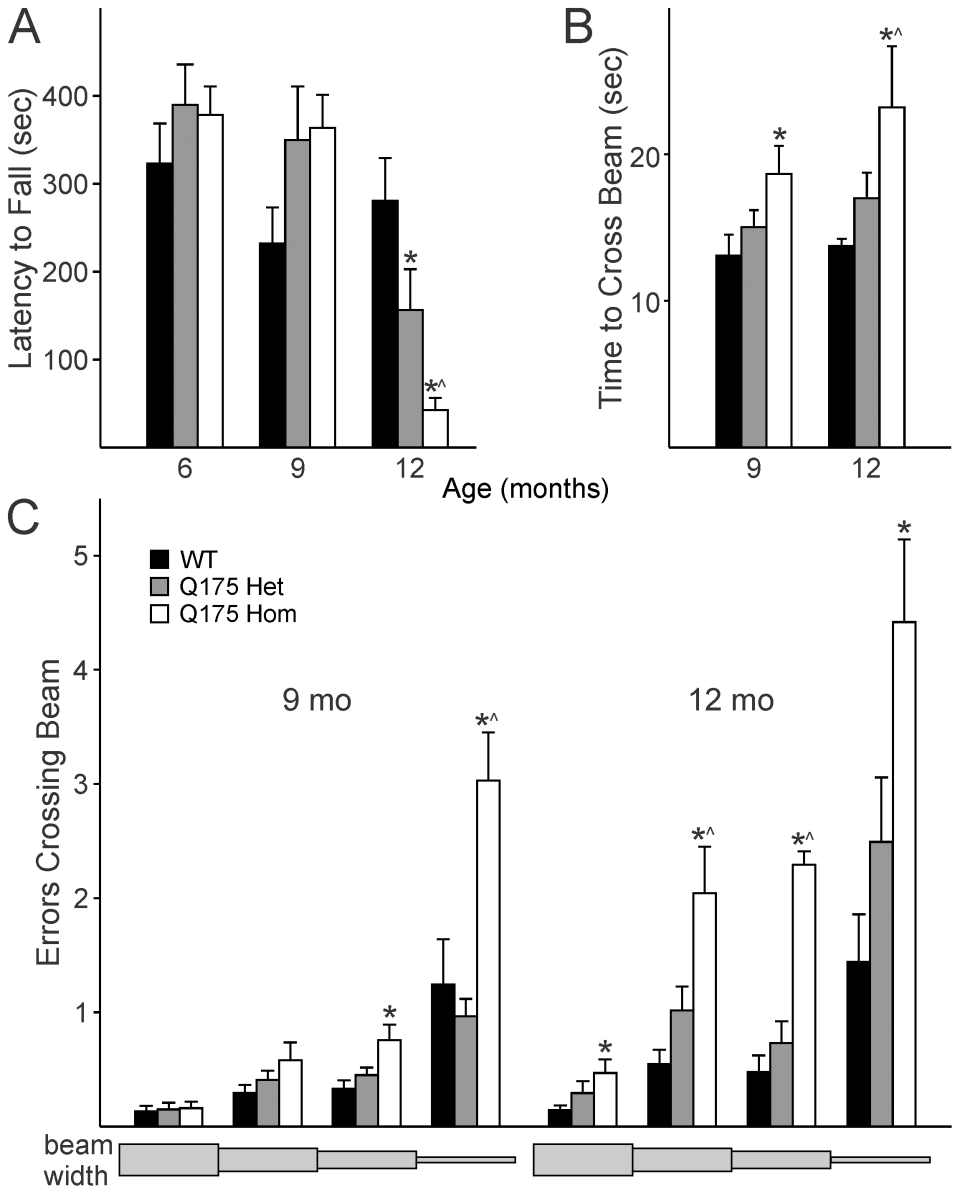

Figure 8: Motor ability of Q175 mutants declines with age.

A. The accelerating rotarod test revealed that the age-related motor deficits in the Q175 model take up to 12 months to appear.

B. 9 month old Q175 Hom mutants take longer to traverse the challenging beam test than age-matched WT and Q175 Het mice.

C. The number of errors made while crossing each segment of the beam are shown, with the widest part of the beam on the left (33 mm) and narrowing towards the right (6 mm). The beam dimensions are not to scale. The number of errors made while crossing the challenging beam are higher in Q175 Hom mutants.

* indicates $P < 0.05$ in post hoc pairwise comparisons with WT after an effect of genotype was detected by one way ANOVA, and ^ indicates differences ($P < 0.05$) between Q175 Het and Hom mice. Reprinted under Creative Commons Attribution License from (Loh et al., 2013)

Q175 mutant mice show deficits in the temporal patterning of sleep

Using video to determine immobility-defined sleep, hourly waveforms of each genotype were generated at the 9 month and 12 month age (figure 9A). The waveforms show a reduction in the nocturnality of the Q175 Hom mice at both ages, replicating the results in wheel running activity. Specifically at 9 and 12 months, Hom mutants spend less time in sleep during the day compared to WT and Het (9 months $F_{2,22} = 8.85$, $P = 0.002$; 12 months $F_{2,22} = 11.42$, $P < 0.001$). An effect of age was confirmed by two way ANOVA comparing daytime sleep across both ages of all three genotypes ($F_{2,45} = 8.12$, $P = 0.007$) in addition to an effect of genotype ($F_{2,45} = 1.13$, $P < 0.001$). Post-hoc pairwise comparisons confirmed a significant difference between WT vs. Q175 Hom ($t_{15} = 4.98$, $P = 0.025$) and Q175 Het vs. Hom ($t_{14} = 5.75$, $P = 0.017$) in total daytime sleep duration.

To examine sleep quality, fragmentation analysis was performed to determine the number of sleep bouts and average bout duration in day versus night. At 9 months, there was no significant difference in the number of daytime sleep bouts (figure 9C top, $F_{2,22} = 1.78$, $P = 0.190$). However, at 12 months of age, increased fragmentation becomes apparent (figure 9C bottom; $F_{2,22} = 5.33$, $P = 0.014$), where the Q175 Hom mice have significantly more daytime sleep bouts than WT mice ($t_{15} = 3.25$, $P = 0.012$). Duration of the average daytime sleep bout is decreased in Q175 Hom mice at 9 months (figure 9D top, $F_{2,22} = 4.99$, $P = 0.020$) and 12 months (figure 9D bottom, $F_{2,22} = 7.90$, $P = 0.003$).

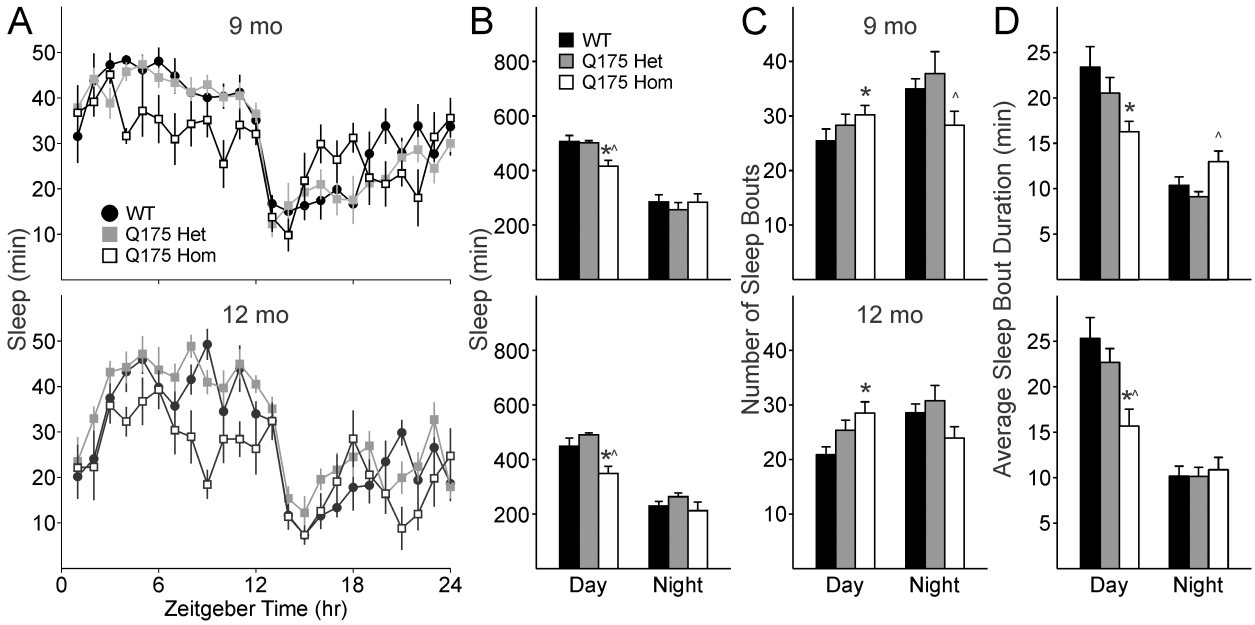

Figure 9: Immobility-defined sleep in the WT, Q175 Het, and Q175 Hom mice at 9 and 12 months of age.
A. Average waveforms of hourly sleep in WT, Q175 Het, and Q175 Hom mice at 9 months (top) and 12 months of age (bottom).
B. Amount of time spent in sleep during day is decreased compared to night-time sleep in Q175 Hom mice at 9 (top) and 12 months of age (bottom).
C. 9 (top) and 12 month (bottom) old Q175 Hom mice have more fragmented daytime sleep, with increased number of sleep episodes.
D. Sleep episodes in Q175 Hom mice are also shorter in duration.
* indicates significant difference ($P < 0.05$) between WT and Q175 Hom mice and ^ indicates differences ($P < 0.05$) between Q175 Het and Hom mice. Reprinted under Creative Commons Attribution License from (Loh et al., 2013)

3-NP

Rhythms in wheel running behavior disrupted in subset of 3-NP treated mice

To determine the effects of the 3-NP toxin on rhythms of behavior, locomotor activity was compared between the 3-NP treated and saline treated mice. Prior to treatments, baseline activity was confirmed to have no differences. Following 3-NP treatment, no statistically significant differences in total activity, power, precision, fragmentation, or free-running period were found. There is, however, an increase in the variability of these parameters. A subset (3 of 10 mice)

developed a disrupted phenotype in their rhythms, with a low power and fragmented rhythm (figure 10, 11).

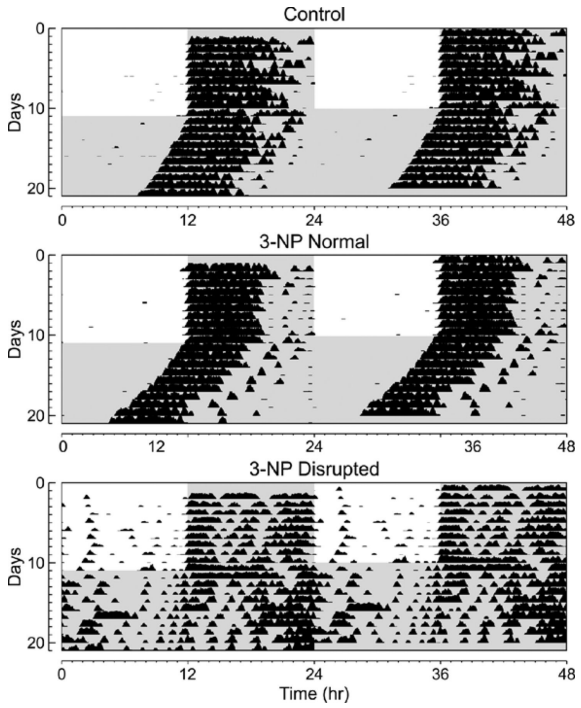

Figure 10: Representative wheel-running behavior of saline-injected and 3-NP-injected mice Each horizontal row represents an activity recorded for a 24-h day. Successive days are double plotted from top to bottom. Shaded panels represent the dark portion of the LD cycle. Top panel: representative wheel-running activity from control mouse held in 12:12 LD for 10 days and then released into DD for 10 days. Middle panel: 3-NP-injected mice with normal activity rhythms. Bottom panel: 3-NP-injected mice with disrupted activity rhythms. Reprinted under Creative Commons Attribution License from (Kudo et al., 2014)

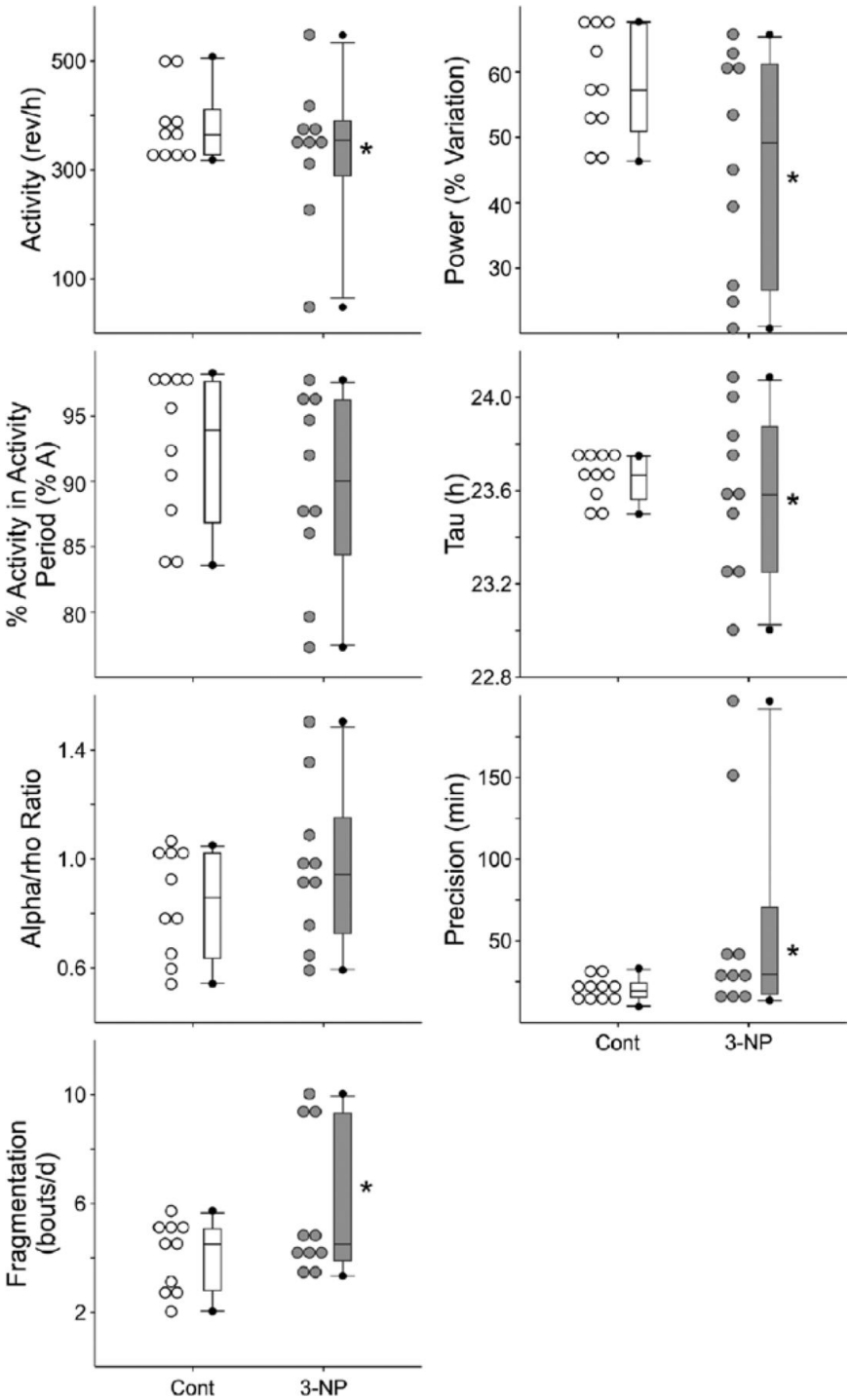

Figure 11: Wheel-running behavior is disrupted in a subset of 3-NP-injected mice
Scatter and box plot of wheel running activity under DD. Overall, no significant reductions in the amount of activity, power, precision, fragmentation or free-running period of the treated mice. On the other hand, there was a significant increase in the variability in key circadian parameters in the 3-NP-treated mice due to a subset of three mice in the 3-NP treated group. * indicates $P < 0.05$, equal variance test compared to controls. Reprinted under Creative Commons Attribution License from (Kudo et al., 2014)

Temporal patterning of immobility-defined sleep is disrupted in 3-NP treated mice

Using video analysis to measure immobility-defined sleep, an average waveform of the 3-NP treated versus saline-treated mice was generated. 3-NP treated mice during the early day showed a lower amount of sleep compared to saline-treated mice (figure 12A). 2 of the 8 3-NP treated mice showed dramatically altered sleep patterning (figure 12B).

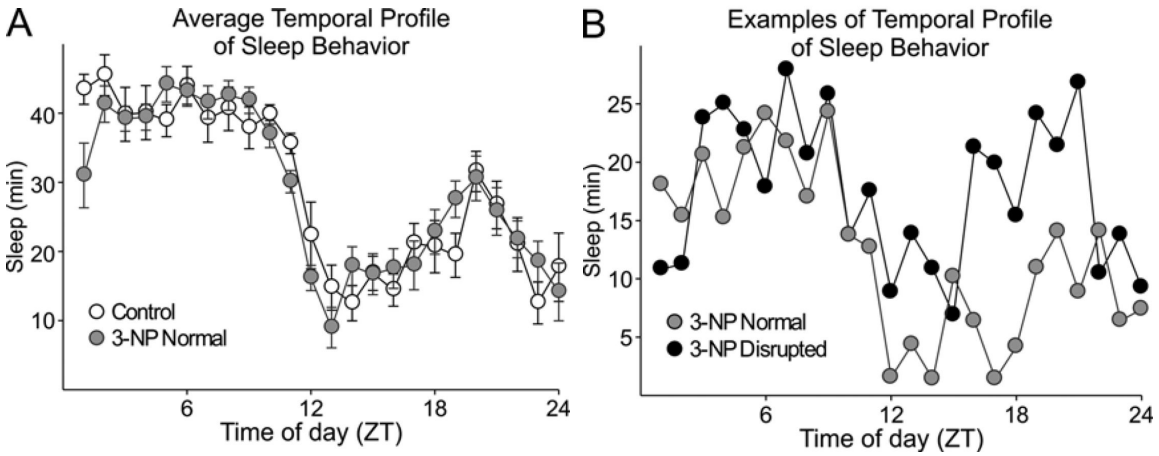

Figure 12: Rhythms in sleep behavior are disrupted in some 3-NP-treated mice
Video recording in combination with an automated mouse tracking analysis software was used to measure sleep behavior. Top panel: average waveforms of the amount (min) of sleep per h between control (n = 8) and 3-NP-treated (n = 8) mice. Overall, we did not see significant differences in the temporal patterning of sleep. Some treated animals had difficulty initiating sleep. Bottom panel: an example of the sleep pattern recorded from a 3-NP-treated mouse with a disrupted sleep rhythm compared with a 3-NP-treated mouse with a normal pattern of sleep.

Conclusion

An assessment of three different mouse models of HD shows that all recapitulate the circadian deficits underlying the sleep/wake disturbances HD patients suffer. Specifically, the BACHD and Q175 mice show imprecise activity onset, lower power of activity rhythms, and increased fragmentation of their activity. These parameters clearly indicate a circadian deficit but the decrease in total activity can partially be attributed to the motor deficits. Further evidence of circadian disruption is seen in their altered patterning of their sleep, with greater fragmentation in the Q175 model during the day and decreased amounts of early-day sleep in the BACHD, Q175, and 3-NP models. This suggests a possibility that it models the difficulty in initiating sleep as HD patients do (Aziz, Anguelova, Marinus, Lammers, & Roos, 2010; Goodman et al., 2011). Further studies using EEG are needed to further assess quality of sleep by detailing the stages of sleep.

In addition, the BACHD and Q175 models recapitulate the motor dysfunction seen in HD, with the BACHD and Q175 mice having a shortened latency to fall on the accelerating rotarod and the Q175 showing a gene-dosage and age-dependent progressive decline in their ability to cross the challenge beam. This is particularly important to note since there is now a clear biomarker of disease progression in the mouse models that can be used to gauge the success of potential treatments for HD.

Other experiments show that there is a deficit in the BACHD's SCN physiology, with altered SCN electrical activity and output. The corresponding reduction of heart rate and body temperature rhythms is likely a consequence of the deficit in SCN output(Kudo et al., 2011). This may explain the desynchronization of SCN and peripheral oscillators as measured by bioluminescent clock gene expression. Evidence from the R6/2 model (Maywood et al., 2010; Pallier et al., 2007) also suggests SCN output is affected. This may be caused by a loss of neuropeptide, vasoactive intestinal peptide (VIP), crucial for the circadian circuitry within the SCN. A decreased amount of

VIP as was shown in the R6/2(Fahrenkrug, Popovic, Georg, Brundin, & Hannibal, 2007) as well as post-mortem study in HD patients(van Wamelen et al., 2013). As VIP is critical for robust rhythms in the SCN(Colwell et al., 2003), a reduction would result in a weakened output and result in deficits consistent with what is seen in the BACHD and Q175 models.

Mitochondrial dysfunction is believed to play a role in the pathology in neurodegenerative diseases(Subramaniam & Chesselet, 2013; Youle & van der Bliek, 2012), and improving mitochondrial function showed evidence in reducing the pathology(Chiang, Chern, & Huang, 2012; Damiano et al., 2013). The subset of 3-NP injected mice with disrupted rhythms showed a similar reduction in daytime firing rate in the SCN, suggesting that a deficiency in energy metabolism may explain the decrease in daytime firing rate in the SCN neurons. Another mechanism in which the circadian and sleep disruptions could accelerate pathology in nervous system is through the misregulation of the reactive oxygen species and inflammation. There is a circadian regulation of antioxidants (Hardeland, Coto-Montes, & Poeggeler, 2003) that could be altered in HD patients.

The next step is to explore treatments to address these deficits such as light therapy or pharmacological interventions like melatonin(Burgess, Sharkey, & Eastman, 2002). Studies have shown evidence in improving motor and cognitive abilities with pharmacological imposition of sleep/wake cycles and light therapy(Maywood et al., 2010; Pallier et al., 2007; Pallier & Morton, 2009).

Chapter 2

Circadian therapies for the BACHD model of Huntington's disease

Introduction

Prior work in the HD mouse models (R6/2 CAG 140, R6/2 CAG 250, Q175 KI, and BACHD) show that they recapitulate the circadian deficits in activity and sleep rhythms in addition to the worsening motor control(Kudo et al., 2011; Loh et al., 2013; Morton et al., 2005). The mice are found to have decreased amplitude and precision in activity rhythms, deficits in SCN neural activity, and the BACHD have dysfunction in physiological outputs in heart rate and body temperature. Consequently, these animals are prime candidates to assess potential treatments targeted at the circadian deficits. Delayed peak in melatonin levels in HD patients at the early stage of the disease further suggests the need for a circadian-based intervention. In addition, prior work has suggested that environmental factors contribute to approximately 40% of the age of HD onset (The U S Venezuela Collaborative et al., 2004). Given the wide range of disease onset for a given CAG repeat length, further studies are needed as to the extent disrupted circadian rhythms worsens the disease and its symptoms.

Currently, there are a variety of potential treatments in circadian medicine ranging from lifestyle changes to pharmacological interventions(Schroeder & Colwell, 2013). Studies in humans have suggested scheduled exercise and meals improve mood and psychiatric disorders (Grandin, Alloy, & Abramson, 2006). Activity, such as exercise, can alter SCN properties and induce changes in clock gene expression and neuronal firing rates, suggesting scheduled exercise being one treatment method. Temporally restricted feeding is also able to reorganize behavior and shift the molecular clock in peripheral tissues (Mistlberger, 2009). Even in a model of poor circadian rhythmicity, the VPAC2 KO mutant mice, their circadian rhythms are entrainable via feeding times despite being nonresponsive to light (Sheward et al., 2007). In addition, a robust photic environment would also boost the cues in which the circadian system uses to synchronize with the environment.

A morning supplemented in blue/green light can send a stronger signal through the ipRGC (intrinsically photosensitive retinal ganglion cells) to better synchronize the peripheral tissues. Finally pharmacological treatments through melatonin or other drugs appear to be promising with the current studies done on Alzheimer's, Parkinson's, and shift workers given their similar deficits in the sleep/wake cycle.

Interventions to enhance circadian rhythms have been shown rescue the HD mouse models' deficits. Work in the R6/2 show progress in rescuing the cognitive and circadian deficits(Maywood et al., 2010; Pallier et al., 2007; Pallier & Morton, 2009). For example, drug and behavioral interventions on a 24-hour cycle improved the R6/2 CAG 250 model's cognitive abilities(Pallier & Morton, 2009). Bright light and scheduled exercise through restricted wheel access improved their rhythmicity and prolonged the duration in which they are rhythmic(Cuesta, Aungier, & Morton, 2014). However the R6/2 model has a very short lifespan and prohibits assessing any physiological changes as a result of these treatments. For this reason, the BACHD mouse model has been chosen to begin a circadian-based treatment as they have a normal lifespan to assess changes in activity, sleep, cognition, and motor performance.

I proposed to rescue the circadian rhythms of the BACHD mouse model with scheduled meals. The mice were screened presymptomatically at 3 months of age to assess their sleep patterning, cognition through the novel object recognition test, and motor ability. Then two cohorts were placed into two treatment protocols: 6 hours feeding during active period (aligned feeding, n=8) and 6 hours feeding during rest period (misaligned feeding, n=8). After 3 months in these two conditions, I reassessed their sleep patterning, cognition, and motor ability. By strengthening the circadian rhythms of the BACHD mice, I hypothesize that the progression of the HD symptoms will be slowed at the post-symptomatic age of 6 months. I believe that aligned feeding is best for rescuing their circadian phenotype while the misaligned feeding conditions will worsen their

phenotype.

Methods

Housing conditions

Adult male mice (BACHD *n*=16) at 8 weeks of age were singly housed in cages and locomotor activity was recorded as previously described (Colwell et al., 2003) using infrared sensors. The BACHD mutants were obtained from the mouse mutant resource at JAX (The Jackson Laboratory, Bar Harbor, Maine) in a colony maintained by the CHDI Foundation. Mice were entrained to a 12:12 hr light:dark (LD) cycle for a minimum of 2 weeks prior to collection of data or beginning treatment. Animals were assessed for motor performance, cognition, and sleep patterning between 2-3 months of age prior to beginning treatments. They are reassessed at 6 months of age after 3 months of continuous treatment.

Treatment conditions

Animals under the aligned feeding conditions (*n*=8) were given standard mouse chow (Teklad 7013) from Zeitgeber time (ZT) 14-20, where ZT=0 is defined as time as lights on. Animals under the misaligned feeding conditions (*n*=8) were given standard mouse chow from ZT 2-8. Both of these conditions allowed the animals to eat at a maintenance level of body weight with no caloric restriction.

Motor tests

The accelerating rotarod test and challenge beam, as described earlier in the methods of Chapter 1, were used to determine the progression of motor dysfunction in the BACHD mice at 3 and 6 months of age. All tests were performed ZT 21 under dim red light to minimize effects of sleep deprivation and light's inhibition of activity.

Immobility-defined sleep

The BACHD mice had their sleep patterning recorded using ANY-maze as described earlier in the methods of Chapter 1.

Novel object recognition

The novel object recognition (NOR) tests were run in ZT 21 under dim red light. Animals were individually placed in a large arena (3 feet X 4 feet) on the first day to habituate for 10 minutes. On days 2-3, the mice were trained using two identical objects for 10 minutes. A camera was mounted directly above the arenas to track the animals. Using the ANY-maze software on days 4-5, the animals were tested by changing one object with a novel object. They were given 5 minutes to explore the arena. The animals are tracked and scored for their duration in which they spend with each object. A discrimination index (DI) of 0.5 means they spend equal amount of time with both objects. A higher DI indicates they favor the novel object over the other familiar object.

Statistical methods

First, we test our data for normality using Shipiro-Wilk. Should we reject the hypothesis of normality, we report the estimated central tendency as medians. Variability is reported as MADAM (Median Absolute Deviation Around the Median). Values are reported as median ± MADAM.

Then a 2-way ANOVA was used to test the variation between and within groups before and after treatment (factor=time), and treatment conditions (aligned feeding or misaligned feeding, factor=treatment), or an interaction between the two factors. Assumptions made for ANOVA include: each sample is an independent observation, the distributions are Gaussian and have equal variance, and the groups are balanced with equal *n*. We assume same underlying population with equal variance, as the animals are in-bred and of the same genotype. Should we reject the null hypothesis with a false positive rate set to α=0.05, we used a post-hoc pairwise multiple comparison with Tukey Honest Significance Difference method to control for false positives due to multiple testing. SigmaStat (version 3.5, SYSTAT Software, San Jose, CA) was used to run statistical analyses.

Results

Cage activity

Between the aligned and misaligned treatment groups, change in free running period (tau) was not significant ($P = 0.505$), change in total activity per day was not significant ($P = 0.219$), change in fragmentation (bouts per day) was not significant ($P = 0.223$), and change in precision of activity onset was not significant ($P = 0.0821$). Under aligned feeding, there was an increase in the nocturnality of the mice ($P = 0.024$) and increased power of rhythms (%V) ($P = 0.001$).

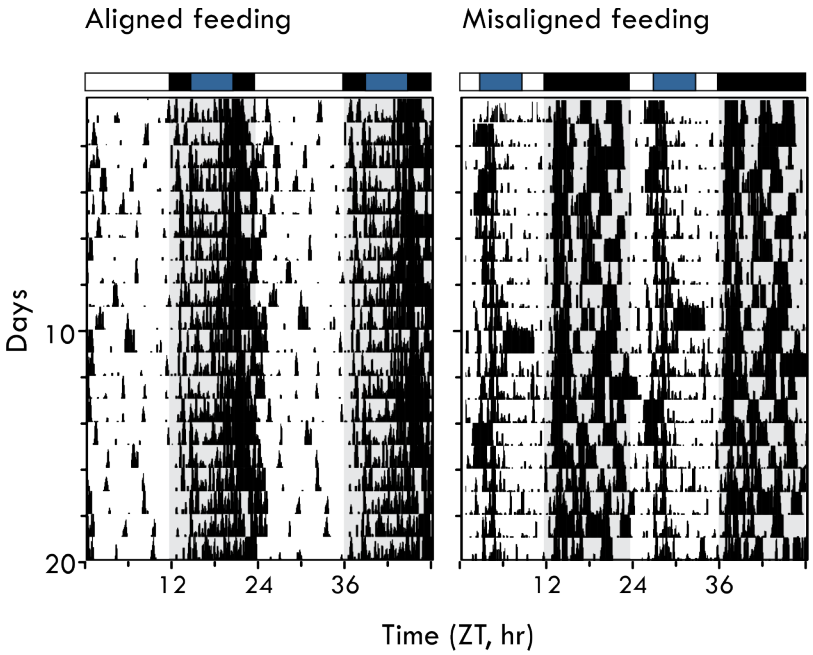

Figure 13: Representative actograms of cage activity as measured by infrared sensors. Figures are double plotted, with top bars indicating the light dark cycles. Dark periods are shaded in gray and feeding times are shaded in blue.

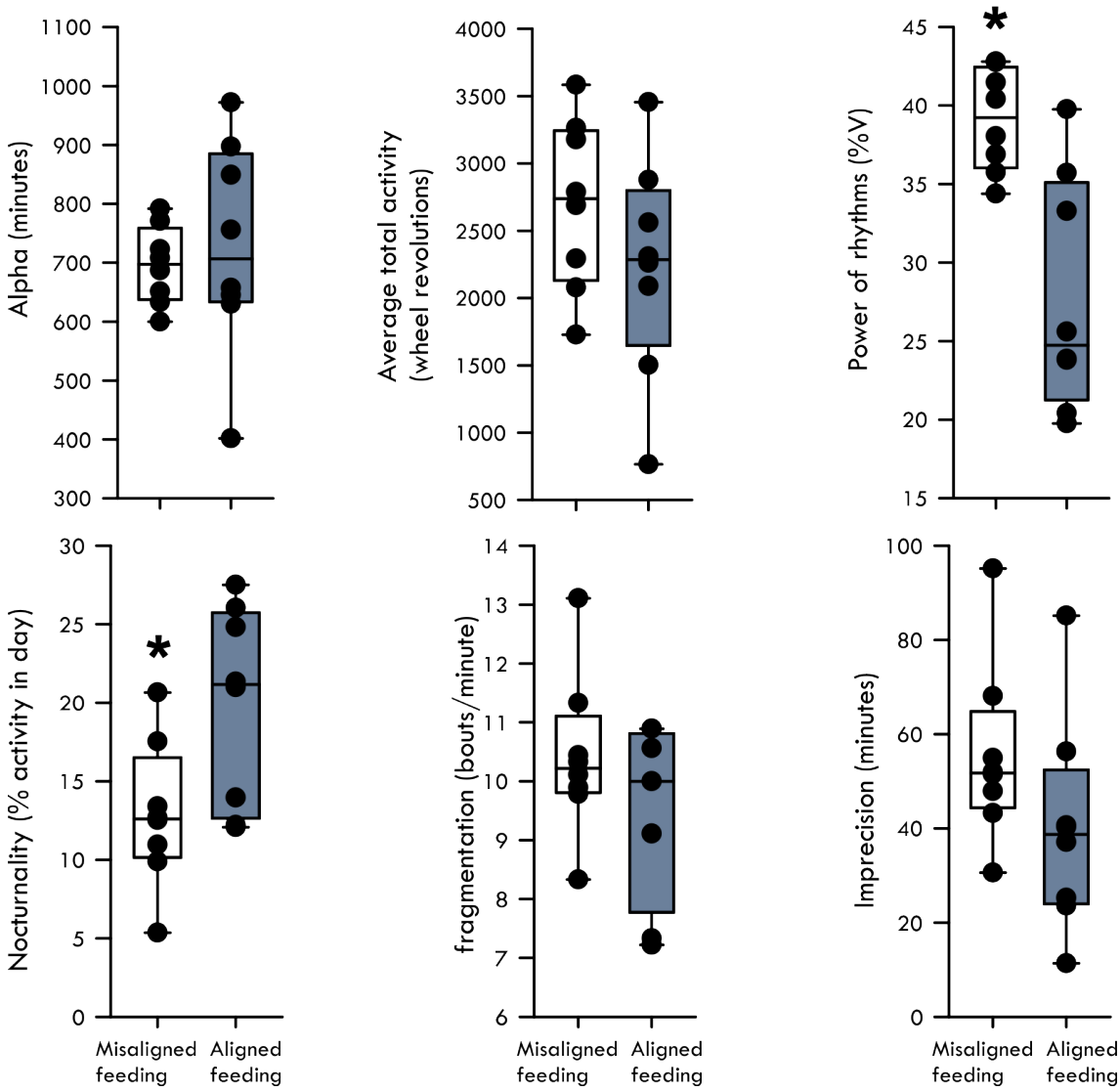

Figure 14: Changes in circadian parameters in the BACHD mutants under aligned or misaligned feeding protocols. Improvements are seen in the nocturnality ($p = 0.024$) and power of rhythms ($P = 0.001$) in the mice under aligned feeding. * indicates statistical significance in a t-test of $P < 0.05$.

Immobility-defined sleep

Total sleep is increased during scheduled feeding

The misaligned feeding mice under baseline conditions had a sleep duration of 593.2 ± 51.89 minutes per day. After being treated for 3 months under misaligned feeding, they had a sleep duration of 720.9 ± 40.09 minutes per day. The aligned feeding mice under baseline conditions had

a sleep duration of 591.3 ± 23.45 minutes per day. After being treated for 3 months under aligned feeding, they had a sleep duration of 693.5 ± 9.625 minutes per day.

A 2-way ANOVA on the total amount of sleep per day failed to reject the null hypothesis for the effect of treatment (F=0.014, P =0.561), or an interaction of time and treatment (F=0.013, P =0.537). Null hypothesis for the effect of time is rejected, where there is an effect of post-treatment on the total amount of sleep for both groups (F=1.398, P <0.001). A post-hoc pairwise comparison with Tukey HSD showed a difference between baseline versus post-treatment aligned feeding groups (p = 0.0023) and a difference between baseline versus post-treatment misaligned feeding groups (p = 0.0002).

Number of sleep bouts

A 2-way ANOVA was performed on the number of sleep bouts. Should an effect of treatment, time, or an interaction between the two is found, a post-hoc pairwise comparison was performed. For the day, an effect of treatment (P = 0.034) and slight effect of time (P = 0.07) was found. For the night, an effect of time (P < 0.001) was found. Mice under aligned feeding during the night show an increase in the number of sleep bouts (baseline aligned: 21.0 ± 1.5; post-treat aligned: 42.25 ± 5.5; P < 0.001). Misaligned feeding shows an increase in sleep bouts during the day (baseline misaligned: 25.75 ± 2.0; post-treat misaligned: 31.75 ± 3.0; P = 0.037) and night (baseline misaligned: 21.0 ± 1.5; post-treat misaligned: 42.25 ± 5.5; P = 0.009).

Sleep bout duration

A 2-way ANOVA was performed on the sleep bout duration. Should an effect of treatment, time, or an interaction between the two is found, a post-hoc pairwise comparison was performed. For the day, an effect of treatment (P = 0.003) and an interaction between time and treatment (P = 0.005) was found. For the night, an effect of treatment (P = 0.002) and an interaction between time and treatment (P < 0.001) was found. The mice under aligned feeding show an increase in the

daytime sleep bout duration (baseline aligned: 18.34 ± 1.07; post-treat aligned: 28.01 ± 5.67; P = 0.015). The misaligned mice had a slightly shorter, but non-significant, sleep bout duration in the day (baseline misaligned: 18.24 ± 2.54; post-treat misaligned: 14.83 ± 1.18; P = 0.091). During night, the converse is true: shorter bouts for the aligned mice (baseline aligned: 10.75 ± 0.91, post-treat aligned: 5.31 ± 0.60; $P < 0.001$) and longer bouts for the misaligned mice (baseline misaligned: 9.01 ± 2.51; post-treat misaligned: 11.70 ± 1.76; P = 0.019).

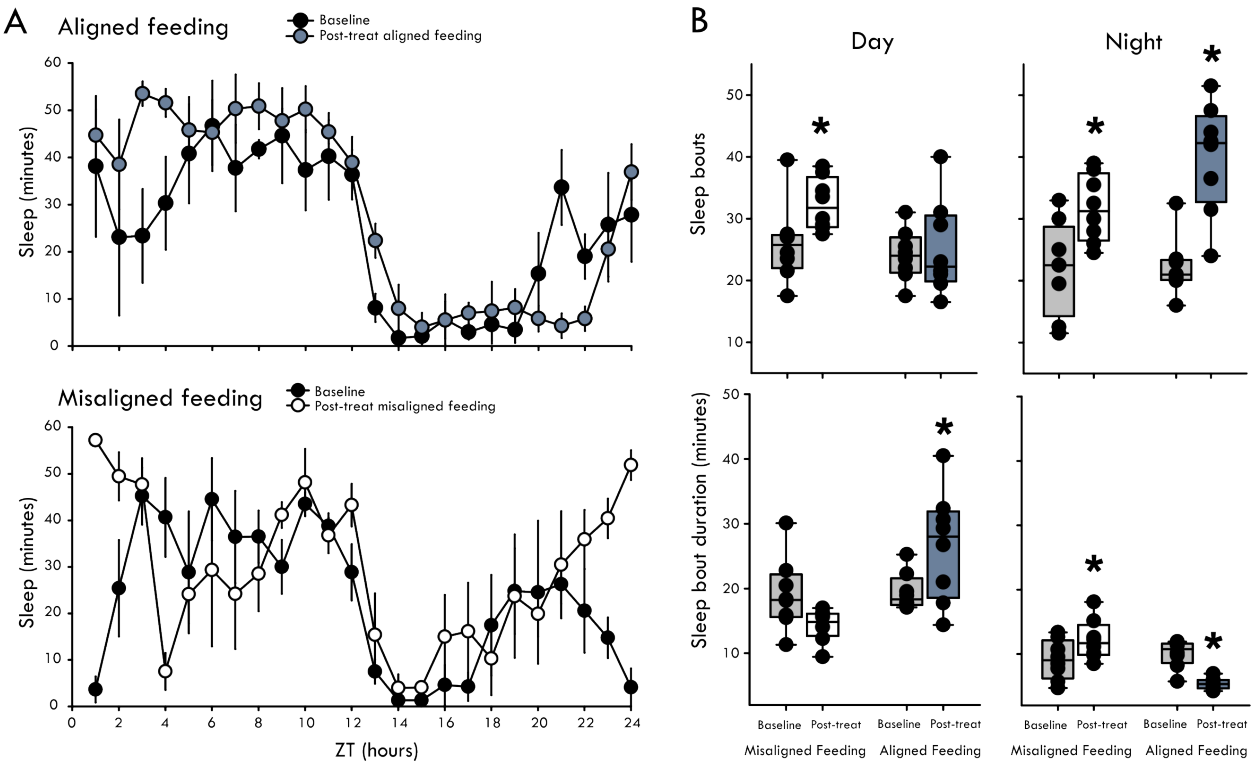

Figure 15: A comparison of total sleep in a 24-hour duration for BACHD animals in baseline groups and post-treatment groups.
A: Improvements in sleep quality are seen in the waveform, with greater early day sleep in both feeding schedules.
B: The mice under aligned feeding show same number of sleep bouts and greater duration of sleep during the day, indicating less fragmented sleep. * indicates a post-hoc test showed $P < 0.05$ between baseline and post-treatment conditions.

Motor tests

Accelerating rotarod test showed no changes between the groups post-treatment

The misaligned feeding mice under baseline conditions spent 209.1 ± 66.8 seconds on the rotarod. After being treated for 3 months under misaligned feeding, they spent 258.1 ± 96.1 seconds on the rotarod. The aligned feeding mice under baseline conditions had a median performance of 199.9 ± 62.3 seconds on the rotarod. After being treated for 3 months under aligned feeding, they spent 209.0 ± 62 seconds on the rotarod.

A 2-way ANOVA was performed to assess whether there is an effect of either time (baseline versus post-treatment) or treatment (misaligned feeding, aligned feeding). The test failed to reject the null hypothesis for the effect of time ($F = 0.610$, $P = 0.444$), effect of treatment ($F=0.375$, $P =0.692$), or an interaction of time and treatment ($F = 2.337$, $P = 0.124$).

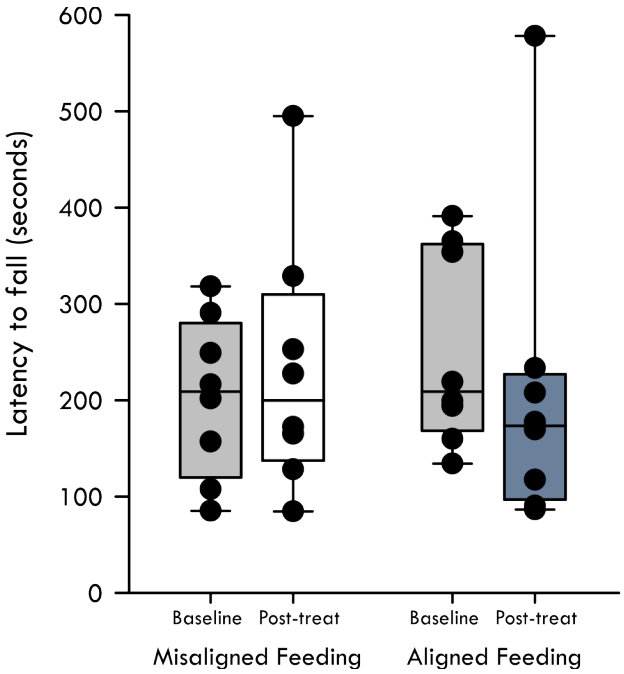

Figure 16: Performance on the accelerating rotarod in the BACHD animals under baseline and post-treatment of aligned or misaligned feeding. Accelerating rotarod test showed no effect of time or treatment.

Challenge beam test showed varied effects due to scheduled meals

The scheduled meals had a treatment effect on the time to cross beam ($P = 0.044$). The total steps to cross beam increased in both post-treatment groups with an effect of time ($P < 0.001$). The number of errors decreased in the misaligned group but increased in the aligned feeding group, with an effect of time ($P = 0.006$) and an interaction between time and treatment ($P < 0.001$).

A more detailed look at the number of steps per segment of the challenge beam showed that the mice in the post-treatment conditions increased their number of steps, regardless of feeding protocol. A 3-way ANOVA revealed an effect of time ($P < 0.001$), segment of beam ($P < 0.001$), and an interaction between treatment and time ($P < 0.055$).

The number of errors per segment of the challenge beam showed that mice in both treatment groups made the most errors in the last segment of the challenge beam, even under baseline conditions. A 3-way ANOVA revealed an effect of time ($P < 0.001$), segment of beam ($P < 0.001$), and an interaction between treatment and time ($P < 0.055$).

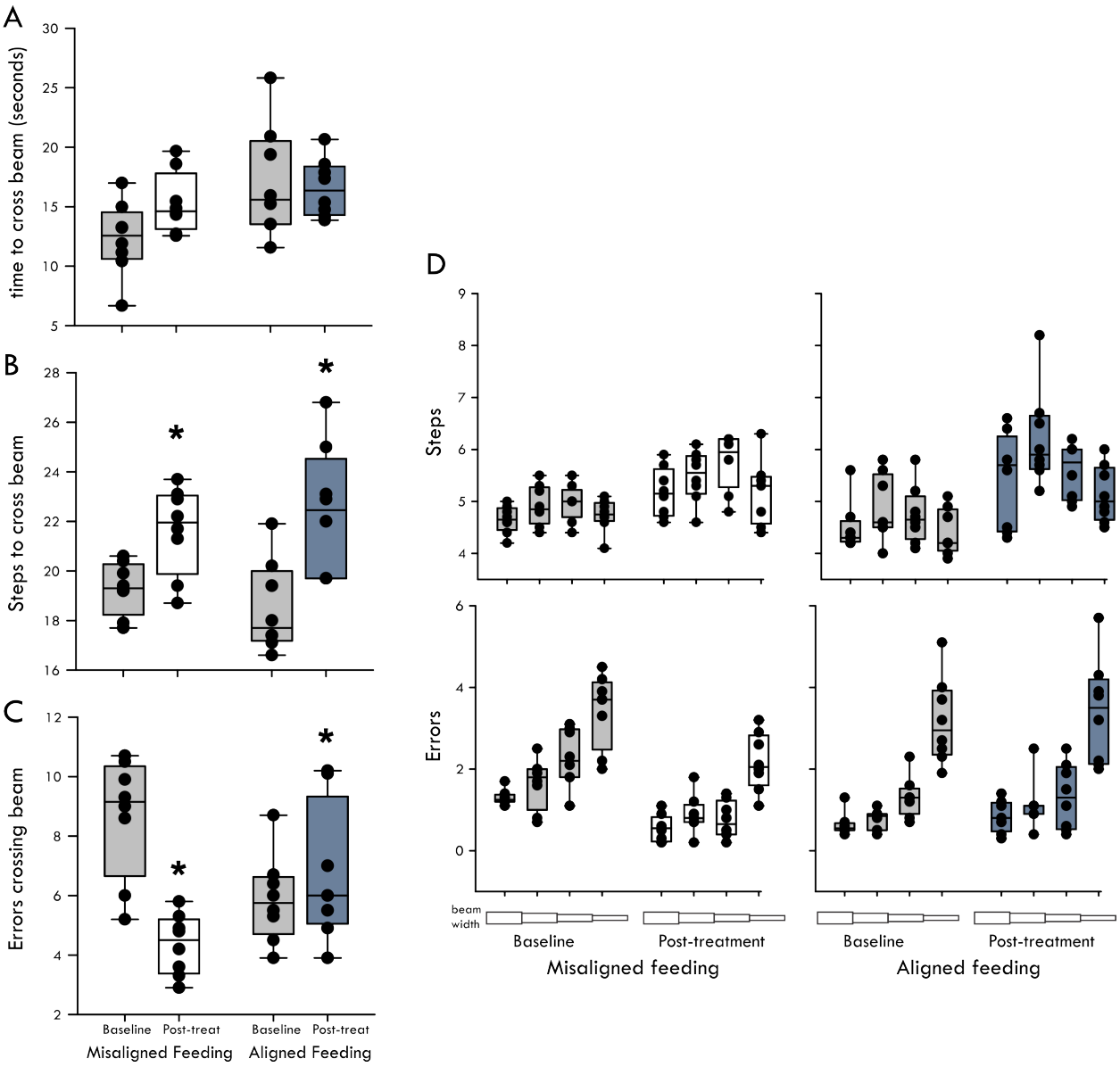

Figure 17: A comparison of performance on the challenge beam motor tests for BACHD animals in baseline groups and post-treatment groups.

Figure A: Time to cross beam

Figure B: Number of steps to cross beam increased under both feeding conditions.

Figure C: Number of errors while crossing beam decreased under misaligned feeding and increased under aligned feeding.

Figure D: Number of steps and errors while crossing beam separated into the beam's four segments, from widest to narrowest as indicated by the diagram.

* indicates a post-hoc test showed $P < 0.05$ between baseline and post-treatment conditions.

Novel object recognition

The misaligned feeding mice under baseline conditions had a median discrimination index of 0.463 ± 0.101. After being treated for 3 months under misaligned feeding, they had a median discrimination index of 0.623 ± 0.162. The aligned feeding mice under baseline conditions had a median discrimination index of 0.604 ± 0.154. After being treated for 3 months under aligned feeding, they had a median discrimination index 0.726 ± 0.026. Effect size of baseline versus post-treatment is an increase of 0.121 (-0.044, 0.305).

A 2-way ANOVA on the discrimination index failed to reject the null hypothesis for the effect of treatment ($F = 3.380$, $P = 0.055$), or an interaction of time and treatment ($F = 0.042$, $P = 0.959$). I can reject the null hypothesis for the effect of time, where there is an effect of post-treatment on the discrimination index for both groups ($F = 6.801$, $P = 0.017$). A post-hoc pairwise comparison with Tukey HSD showed a difference between baseline and post-treatment groups ($P = 0.017$).

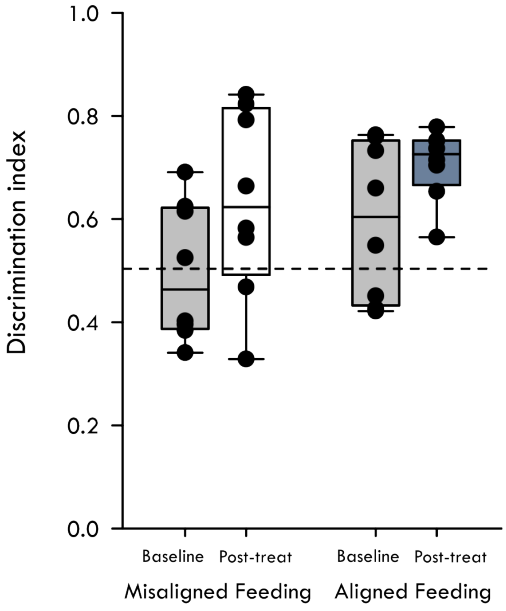

Figure 18: A comparison of performance on the novel object recognition task for BACHD animals in baseline groups and post-treatment groups. No effects were found for time or treatment.

Conclusion

In this study, I found that scheduled mealtime offers an improvement in various circadian parameters in cage activity and sleep patterning. The cage activity rhythms show a reduction in the activity during light (an increase in nocturnality) as well as an increase in the power of rhythms for mice under aligned feeding. In addition, the sleep pattern of BACHD mice is shown here to be malleable, changing accordingly to more closely resemble WT mice under same feeding protocols. Improvement in sleep was seen through restoration of sleep during the early day and decreased fragmentation of daytime sleep (fewer bouts and longer bout duration) when mice were under aligned feeding. Total amount of sleep was also increased under both conditions. In addition to the improvements in circadian parameters, the motor and cognitive abilities of the BACHD mice showed no further decline in the scheduled meal conditions. Scheduled feeding delayed the age-dependent decline in motor activity but did not restore motor function to the levels seen in WT controls. The full extent of the impact of scheduled feeding on motor performance waits one critical control group i.e. we do not have the data for BACHD animals under ad libitum feeding to assess the changes from 3 months to 6 months of age in their sleep, cognition, and motor performance without scheduled meals. The results of this group must be obtained before publication of the findings.

The circadian system is strongly linked with metabolic homeostasis by regulating the daily rhythms of processes such as appetite, gastrointestinal function, and pancreatic insulin secretion(Bass, 2012; Froy, 2010; Hoogerwerf, 2006). The SCN's role as the central pacemaker allows coordination of the molecular clocks in metabolic tissues such as the liver and pancreas(Cailotto et al., 2005; Guo, Brewer, Champhekar, Harris, & Bittman, 2005; Shibata, 2004). Clock genes (*Bmal1* and *Clock*) and nuclear hormone receptors (*Rev-erb* α and *Ror* α) in the peripheral tissues modulate metabolic pathways, enabling the circadian system to directly affect metabolism.

Disrupting the circadian system through genetic or environmental manipulations leads to the loss of rhythms in clock and metabolic genes in the liver and pancreas, depressing the genes' absolute expression levels (Barclay et al., 2012; Paschos et al., 2012; Qian, Block, Colwell, & Matveyenko, 2013; Shimba et al., 2011; Turek et al., 2005). Circadian dysfunction often results in pathologies consistent with metabolic syndrome, including hypoinsulinemia, hyperglycemia, and obesity (Coomans et al., 2013; Gale et al., 2011; Rudic et al., 2004; Turek et al., 2005). In humans, short-term circadian misalignment is sufficient to produce pre-diabetic conditions in the body (Scheer et al., 2009; Leproult et al., 2014), and long-term disruptions in the sleep/wake cycle leads to metabolic disruptions (Markwald et al., 2013; Spiegel, Tasali, Leproult, & Van Cauter, 2009).

The metabolic pathway, on the other hand, can also interact with the molecular clock, enabling a response from the circadian system to balance energy intake and expenditure. For example, frequency and volume of food intake (Hirao et al., 2010; Kuroda et al., 2012), as well as the nutrient composition of the food, has been shown to alter the circadian function (Hatori et al., 2012; Kohsaka et al., 2007; Oishi, Uchida, & Itoh, 2012). Disruptive feeding conditions can result in circadian dysfunction and metabolic imbalances (Arble, Bass, Laposky, Vitaterna, & Turek, 2009; L. Wu & Reddy, 2013). Food access restricted to mice and rats' normal sleep phase shifts the phase of the molecular clock in peripheral tissues including the liver, adrenals, and fat cells, but not in the SCN (Damiola et al., 2000; Stokkan, Yamazaki, Tei, Sakaki, & Menaker, 2001). Consequently, the misalignment of rhythms between peripheral and the SCN can lead to altered expression of metabolic enzymes, changes in energy balance, and weight gain (Bray et al., 2013; Karatsoreos, Bhagat, Bloss, Morrison, & McEwen, 2011). Not only can temporally manipulating food access change clock gene expression, but also the composition of the food can have adverse effects. Rodents fed a high fat diet (HFD) that ate the same amount of calories as those on normal chow exhibited changes in behavioral periodicity, disrupted molecular clocks in the beta cells of pancreas

and liver, changes to rhythms in metabolic genes in liver, impaired insulin secretion, and increase in weight (Hatori et al., 2012; Kohsaka et al., 2007; Vieira et al., 2012). These signs of metabolic syndrome are reversed when the HFD is restricted to 8 hours in the middle of their active period (Hatori et al., 2012; Sherman et al., 2012). In mice lacking a functional molecular clock (Cry1,2 dKO), scheduled feeding can restore rhythms of most clock and metabolic genes in the liver and prevent weight gain (Vollmers et al., 2009). These studies suggest that metabolic homeostasis is dependent on an intact circadian system and an appropriate time of feeding.

Given the interaction between the circadian system and metabolism, a feeding schedule that reinforces the phase relationship of clock gene expression between the central and peripheral clocks may be a crucial lifestyle for maintaining good health. In aging and neurodegenerative diseases where SCN communication with peripheral tissues is deficient, scheduled feeding may supply the necessary cues to properly realign molecular rhythms among tissues. For example in mouse models of Huntington's disease, scheduled feeding appears to be able to entrain the peripheral tissues (Maywood et al., 2010). In humans, higher measures of daily routine such as mealtimes, is correlated with higher self-reported sleep quality (Câmara Magalhães, Vitorino Souza, Rocha Dias, Felipe Carvalhedo de Bruin, & de Bruin, 2005; Frank et al., 1997; Monk, Petrie, Hayes, & Kupfer, 1994; Zisberg, Gur-Yaish, & Shochat, 2010). Whether the timing of food consumption within the active period matters is yet to be elucidated. One example is seen in Alzheimer's disease, where the peak of calorie intake is phase advanced. These shifts in timing are correlated with lower body weights and worse cognitive and behavioral symptoms(Young & Greenwood, 2001), suggesting a relationship between timing of food intake and severity of disease. Much more work will need to be done to clarify the benefits of scheduled feeding including its potential to realign the circadian system and whether this may help disease symptoms. My results suggest that scheduled meals can be a promising lifestyle-based treatment for prolonging the quality of life for patients suffering from

Huntington's disease. This methodology offers a safe and effective treatment in improving the sleep quality and improving their circadian rhythms.

Bibliography

Arble, D. M., Bass, J., Laposky, A. D., Vitaterna, M. H., & Turek, F. W. (2009). Circadian timing of food intake contributes to weight gain. *Obesity (Silver Spring, Md.)*, *17*(11), 2100–2102. doi:10.1038/oby.2009.264

Aziz, N. A., Anguelova, G. V., Marinus, J., Lammers, G. J., & Roos, R. A. C. (2010). Sleep and circadian rhythm alterations correlate with depression and cognitive impairment in Huntington's disease. *Parkinsonism & Related Disorders*, *16*(5), 345–350. doi:10.1016/j.parkreldis.2010.02.009

Barclay, J. L., Husse, J., Bode, B., Naujokat, N., Meyer-Kovac, J., Schmid, S. M., et al. (2012). Circadian desynchrony promotes metabolic disruption in a mouse model of shiftwork. *PloS One*, *7*(5), e37150. doi:10.1371/journal.pone.0037150

Bass, J. (2012). Circadian topology of metabolism. *Nature*, *491*(7424), 348–356. doi:10.1038/nature11704

Bray, M. S., Ratcliffe, W. F., Grenett, M. H., Brewer, R. A., Gamble, K. L., & Young, M. E. (2013). Quantitative analysis of light-phase restricted feeding reveals metabolic dyssynchrony in mice. *International Journal of Obesity (2005)*, *37*(6), 843–852. doi:10.1038/ijo.2012.137

Brouillet, E. (2014). The 3-NP Model of Striatal Neurodegeneration. *Current Protocols in Neuroscience / Editorial Board, Jacqueline N. Crawley ... [Et Al.]*, *67*, 9.48.1–9.48.14. doi:10.1002/0471142301.ns0948s67

Burgess, H. J., Sharkey, K. M., & Eastman, C. I. (2002). Bright light, dark and melatonin can promote circadian adaptation in night shift workers. *Sleep Medicine Reviews*, *6*(5), 407–420.

Cailotto, C., La Fleur, S. E., Van Heijningen, C., Wortel, J., Kalsbeek, A., Feenstra, M., et al. (2005). The suprachiasmatic nucleus controls the daily variation of plasma glucose via the autonomic output to the liver: are the clock genes involved? *The European Journal of Neuroscience*, *22*(10), 2531–2540. doi:10.1111/j.1460-9568.2005.04439.x

Campbell, S. S., & Tobler, I. (1984). Animal sleep: a review of sleep duration across phylogeny. *Neuroscience and Biobehavioral Reviews*.

Câmara Magalhães, S., Vitorino Souza, C., Rocha Dias, T., Felipe Carvalhedo de Bruin, P., & de Bruin, V. M. S. (2005). Lifestyle regularity measured by the social rhythm metric in Parkinson's disease. *Chronobiology International*, *22*(5), 917–924. doi:10.1080/07420520500263334

Chiang, M.-C., Chern, Y., & Huang, R.-N. (2012). PPARgamma rescue of the mitochondrial dysfunction in Huntington's disease. *Neurobiology of Disease*, *45*(1), 322–328. doi:10.1016/j.nbd.2011.08.016

Colwell, C. S., Michel, S., Itri, J., Rodriguez, W., Tam, J., Lelievre, V., et al. (2003). Disrupted circadian rhythms in VIP- and PHI-deficient mice. *American Journal of Physiology Regulatory, Integrative and Comparative Physiology*, *285*(5), R939–49. doi:10.1152/ajpregu.00200.2003

Coomans, C. P., van den Berg, S. A. A., Houben, T., van Klinken, J.-B., van den Berg, R., Pronk, A. C. M., et al. (2013). Detrimental effects of constant light exposure and high-fat diet on circadian energy metabolism and insulin sensitivity. *FASEB Journal : Official Publication of the Federation of American Societies for Experimental Biology*, *27*(4), 1721–1732. doi:10.1096/fj.12-210898

Cuesta, M., Aungier, J., & Morton, A. J. (2014). Neurobiology of Disease. *Neurobiology of Disease*, *63*(C), 85–91. doi:10.1016/j.nbd.2013.11.008

Damiano, M., Diguet, E., Malgorn, C., D'Aurelio, M., Galvan, L., Petit, F., et al. (2013). A role of mitochondrial complex II defects in genetic models of Huntington's disease expressing N-terminal fragments of mutant huntingtin. *Human Molecular Genetics*, *22*(19), 3869–3882. doi:10.1093/hmg/ddt242

Damiola, F., Le Minh, N., Preitner, N., Kornmann, B., Fleury-Olela, F., & Schibler, U. (2000). Restricted feeding uncouples circadian oscillators in peripheral tissues from the central pacemaker in the suprachiasmatic nucleus. *Genes & Development*, *14*(23), 2950–2961.

Dibner, C., Schibler, U., & Albrecht, U. (2010). The mammalian circadian timing system: organization and coordination of central and peripheral clocks. *Annual Review of Physiology*, *72*, 517–549. doi:10.1146/annurev-physiol-021909-135821

Fahrenkrug, J., Popovic, N., Georg, B., Brundin, P., & Hannibal, J. (2007). Decreased VIP and VPAC2 receptor expression in the biological clock of the R6/2 Huntington's disease mouse. *Journal of Molecular Neuroscience : MN*, *31*(2), 139–148.

Fisher, S. P., Godinho, S. I. H., Pothecary, C. A., Hankins, M. W., Foster, R. G., & Peirson, S. N. (2012). Rapid assessment of sleep-wake behavior in mice. *Journal of Biological Rhythms*, *27*(1), 48–58. doi:10.1177/0748730411431550

Fleming, S. M., Salcedo, J., & Fernagut, P. O. (2004). Early and progressive sensorimotor anomalies in mice overexpressing wild-type human ***α***-synuclein. *The Journal of* ….

Frank, E., Hlastala, S., Ritenour, A., Houck, P., Tu, X. M., Monk, T. H., et al. (1997). Inducing lifestyle regularity in recovering bipolar disorder patients: results from the maintenance therapies in bipolar disorder protocol. *Biological Psychiatry*, *41*(12), 1165–1173.

Froy, O. (2010). Metabolism and circadian rhythms--implications for obesity. *Endocrine Reviews*, *31*(1), 1–24. doi:10.1210/er.2009-0014

Gale, J. E., Cox, H. I., Qian, J., Block, G. D., Colwell, C. S., & Matveyenko, A. V. (2011). Disruption of circadian rhythms accelerates development of diabetes through pancreatic beta-cell loss and dysfunction. *Journal of Biological Rhythms*, *26*(5), 423–433. doi:10.1177/0748730411416341

Goodman, A. O. G., & Barker, R. A. (2010). How vital is sleep in Huntington's disease? *Journal of Neurology*, *257*(6), 882–897. doi:10.1007/s00415-010-5517-4

Goodman, A. O. G., Rogers, L., Pilsworth, S., McAllister, C. J., Shneerson, J. M., Morton, A. J., & Barker, R. A. (2011). Asymptomatic sleep abnormalities are a common early feature in patients with Huntington's disease. *Current Neurology and Neuroscience Reports*, *11*(2), 211–217. doi:10.1007/s11910-010-0163-x

Grandin, L. D., Alloy, L. B., & Abramson, L. Y. (2006). The social zeitgeber theory, circadian rhythms, and mood disorders: review and evaluation. *Clinical Psychology Review*, *26*(6), 679–694. doi:10.1016/j.cpr.2006.07.001

Gray, M., Shirasaki, D. I., Cepeda, C., André, V. M., Wilburn, B., Lu, X.-H., et al. (2008). Full-Length Human Mutant Huntingtin with a Stable Polyglutamine Repeat Can Elicit Progressive and Selective Neuropathogenesis in BACHD Mice. *The Journal of …*.

Guo, H., Brewer, J. M., Champhekar, A., Harris, R. B. S., & Bittman, E. L. (2005). Differential control of peripheral circadian rhythms by suprachiasmatic-dependent neural signals. *Proceedings of the National Academy of Sciences of the United States of America*, *102*(8), 3111–3116. doi:10.1073/pnas.0409734102

Hardeland, R., Coto-Montes, A., & Poeggeler, B. (2003). Circadian rhythms, oxidative stress, and antioxidative defense mechanisms. *Chronobiology International*, *20*(6), 921–962.

Hatori, M., Vollmers, C., Zarrinpar, A., Ditacchio, L., Bushong, E. A., Gill, S., et al. (2012). Time-Restricted Feeding without Reducing Caloric Intake Prevents Metabolic Diseases in Mice Fed a High-Fat Diet. *Cell Metabolism*, *15*(6), 848–860. doi:10.1016/j.cmet.2012.04.019

Hirao, A., Nagahama, H., Tsuboi, T., Hirao, M., Tahara, Y., & Shibata, S. (2010). Combination of starvation interval and food volume determines the phase of liver circadian rhythm in Per2::Luc knock-in mice under two meals per day feeding. *American Journal of Physiology. Gastrointestinal and Liver Physiology*, *299*(5), G1045–53. doi:10.1152/ajpgi.00330.2010

Hoogerwerf, W. A. (2006). Biologic clocks and the gut. *Current Gastroenterology Reports*, *8*(5), 353–359.

Karatsoreos, I. N., Bhagat, S., Bloss, E. B., Morrison, J. H., & McEwen, B. S. (2011). Disruption of circadian clocks has ramifications for metabolism, brain, and behavior. *Proceedings of the National Academy of Sciences of the United States of America*, *108*(4), 1657–1662. doi:10.1073/pnas.1018375108

Kohsaka, A., Laposky, A. D., Ramsey, K. M., Estrada, C., Joshu, C., Kobayashi, Y., et al. (2007). High-fat diet disrupts behavioral and molecular circadian rhythms in mice. *Cell Metabolism*, *6*(5), 414–421. doi:10.1016/j.cmet.2007.09.006

Kudo, T., Loh, D. H., Tahara, Y., Truong, D., Hernández-Echeagaray, E., & Colwell, C. S. (2014). Circadian dysfunction in response to in vivo treatment with the mitochondrial toxin 3-nitropropionic acid. *ASN Neuro*, *6*(1). doi:10.1042/AN20130042

Kudo, T., Schroeder, A., Loh, D. H., Kuljis, D., Jordan, M. C., Roos, K. P., & Colwell, C. S. (2011). Dysfunctions in circadian behavior and physiology in mouse models of Huntington's disease. *Experimental Neurology*, *228*(1), 80–90. doi:10.1016/j.expneurol.2010.12.011

Kuroda, H., Tahara, Y., Saito, K., Ohnishi, N., Kubo, Y., Seo, Y., et al. (2012). Meal frequency patterns determine the phase of mouse peripheral circadian clocks. *Scientific Reports*, *2*, 711. doi:10.1038/srep00711

Leproult R, Holmbäck U, Van Cauter E. Circadian misalignment augments markers of insulin resistance and inflammation, independently of sleep loss. *Diabetes*. 2014 Jun;63(6):1860-9

Loh, D. H., Kudo, T., Truong, D., Wu, Y., & Colwell, C. S. (2013). The Q175 Mouse Model of Huntington's Disease Shows Gene Dosage- and Age-Related Decline in Circadian Rhythms of Activity and Sleep. *PloS One*, *8*(7), e69993. doi:10.1371/journal.pone.0069993

Loh, D. H., Navarro, J., Hagopian, A., Wang, L. M., Deboer, T., & Colwell, C. S. (2010). Rapid changes in the light/dark cycle disrupt memory of conditioned fear in mice. *PloS One*, *5*(9), e12546. doi:10.1371/journal.pone.0012546.t001

Markwald, R. R., Melanson, E. L., Smith, M. R., Higgins, J., Perreault, L., Eckel, R. H., & Wright, K. P. (2013). Impact of insufficient sleep on total daily energy expenditure, food intake, and weight gain. *Pnas*, *110*(14), 5695–5700. doi:10.1073/pnas.1216951110

Marshall, J., White, K., Weaver, M., Flury Wetherill, L., Hui, S., Stout, J. C., et al. (2007). Specific psychiatric manifestations among preclinical Huntington disease mutation carriers. *Archives of Neurology*, *64*(1), 116–121. doi:10.1001/archneur.64.1.116

Maywood, E. S., Fraenkel, E., McAllister, C. J., Wood, N., Reddy, A. B., Hastings, M. H., & Morton, A. J. (2010). Disruption of peripheral circadian timekeeping in a mouse model of Huntington's disease and its restoration by temporally scheduled feeding. *The Journal of Neuroscience : the Official Journal of the Society for Neuroscience*, *30*(30), 10199–10204. doi:10.1523/JNEUROSCI.1694-10.2010

Mcclung, C. A. (2011). Circadian rhythms and mood regulation: insights from pre-clinical models. *European Neuropsychopharmacology : the Journal of the European College of Neuropsychopharmacology*, *21 Suppl 4*, S683–93. doi:10.1016/j.euroneuro.2011.07.008

Menalled, L. B., Kudwa, A. E., Miller, S., Fitzpatrick, J., Watson-Johnson, J., Keating, N., et al. (2012). Comprehensive Behavioral and Molecular Characterization of a New Knock-In Mouse Model of Huntington's Disease: zQ175. *PloS One*, *7*(12), e49838. doi:10.1371/journal.pone.0049838.t002

Menalled, L., El-Khodor, B. F., Patry, M., Suárez-Fariñas, M., Orenstein, S. J., Zahasky, B., et al. (2009). Systematic behavioral evaluation of Huntington's disease transgenic and knock-in mouse models. *Neurobiology of Disease*, *35*(3), 319–336. doi:10.1016/j.nbd.2009.05.007

Mistlberger, R. E. (2009). Food-anticipatory circadian rhythms: concepts and methods. *The European Journal of Neuroscience*, *30*(9), 1718–1729. doi:10.1111/j.1460-9568.2009.06965.x

Monk, T. H., Petrie, S. R., Hayes, A. J., & Kupfer, D. J. (1994). Regularity of daily life in relation to personality, age, gender, sleep quality and circadian rhythms. *Journal of Sleep Research*, *3*(4), 196–205.

Morton, A. J., Wood, N. I., Hastings, M. H., Hurelbrink, C., Barker, R. A., & Maywood, E. S. (2005). Disintegration of the sleep-wake cycle and circadian timing in Huntington's disease. *The Journal of Neuroscience : the Official Journal of the Society for Neuroscience*, *25*(1), 157–163. doi:10.1523/JNEUROSCI.3842-04.2005

Oishi, K., Uchida, D., & Itoh, N. (2012). Low-carbohydrate, high-protein diet affects rhythmic expression of gluconeogenic regulatory and circadian clock genes in mouse peripheral tissues. *Chronobiology International*, *29*(7), 799–809. doi:10.3109/07420528.2012.699127

Pack, A. I., Galante, R. J., Maislin, G., Cater, J., Metaxas, D., Lu, S., et al. (2007). Novel method for high-throughput phenotyping of sleep in mice.

Pallier, P. N., & Morton, A. J. (2009). Management of sleep/wake cycles improves cognitive function in a transgenic mouse model of Huntington's disease. *Brain Research*.

Pallier, P. N., Maywood, E. S., Zheng, Z., Chesham, J. E., Inyushkin, A. N., Dyball, R., et al. (2007). Pharmacological imposition of sleep slows cognitive decline and reverses dysregulation of circadian gene expression in a transgenic mouse model of Huntington's disease. *The Journal of Neuroscience : the Official Journal of the Society for Neuroscience*, *27*(29), 7869–7878. doi:10.1523/JNEUROSCI.0649-07.2007

Paschos, G. K., Ibrahim, S., Song, W.-L., Kunieda, T., Grant, G., Reyes, T. M., et al. (2012). Obesity in mice with adipocyte-specific deletion of clock component Arntl. *Nature Medicine*, *18*(12), 1768–1777. doi:10.1038/nm.2979

Qian, J., Block, G. D., Colwell, C. S., & Matveyenko, A. V. (2013). Consequences of exposure to light at night on the pancreatic islet circadian clock and function in rats. *Diabetes*, *62*(10), 3469–3478. doi:10.2337/db12-1543

Rudic, R. D., McNamara, P., Curtis, A.-M., Boston, R. C., Panda, S., Hogenesch, J. B., & FitzGerald, G. A. (2004). BMAL1 and CLOCK, two essential components of the circadian clock, are involved in glucose homeostasis. *PLoS Biology*, *2*(11), e377. doi:10.1371/journal.pbio.0020377

Scheer, F. A., Hilton, M. F., Mantzoros, C. S., & Shea, S. A. (2009). Adverse metabolic and cardiovascular consequences of circadian misalignment. *Proceedings of the National Academy of Sciences of the United States of America*, *106*(11), 4453–8. doi:10.1073/pnas.0808180106

Schroeder, A. M., & Colwell, C. S. (2013). How to fix a broken clock. *Trends in Pharmacological Sciences*, *34*(11), 605–619. doi:10.1016/j.tips.2013.09.002

Sherman, H., Genzer, Y., Cohen, R., Chapnik, N., Madar, Z., & Froy, O. (2012). Timed high-fat diet resets circadian metabolism and prevents obesity. *FASEB Journal : Official Publication of the Federation of American Societies for Experimental Biology*, *26*(8), 3493–3502. doi:10.1096/fj.12-208868

Sheward, W. J., Maywood, E. S., French, K. L., Horn, J. M., Hastings, M. H., Seckl, J. R., et al. (2007). Entrainment to Feeding but Not to Light: Circadian Phenotype of VPAC2 Receptor-Null Mice. *The Journal of* ….

Shibata, S. (2004). Neural regulation of the hepatic circadian rhythm. *The Anatomical Record. Part a, Discoveries in Molecular, Cellular, and Evolutionary Biology*, *280*(1), 901–909. doi:10.1002/ar.a.20095

Shimba, S., Ogawa, T., Hitosugi, S., Ichihashi, Y., Nakadaira, Y., Kobayashi, M., et al. (2011). Deficient of a clock gene, brain and muscle Arnt-like protein-1 (BMAL1), induces dyslipidemia and ectopic fat formation. *PloS One*, *6*(9), e25231. doi:10.1371/journal.pone.0025231

Sokolove, P. G., & Bushell, W. N. (1978). The chi square periodogram: its utility for analysis of circadian rhythms. *Journal of Theoretical Biology*, *72*(1), 131–160.

Spiegel, K., Tasali, E., Leproult, R., & Van Cauter, E. (2009). Effects of poor and short sleep on glucose metabolism and obesity risk. *Nature Reviews. Endocrinology*, *5*(5), 253–261. doi:10.1038/nrendo.2009.23

Stokkan, K. A., Yamazaki, S., Tei, H., Sakaki, Y., & Menaker, M. (2001). Entrainment of the circadian clock in the liver by feeding. *Science (New York, N.Y.)*, *291*(5503), 490–493. doi:10.1126/science.291.5503.490

Stout, J. C., Paulsen, J. S., Queller, S., Solomon, A. C., Whitlock, K. B., Campbell, J. C., et al. (2011). Neurocognitive signs in prodromal Huntington disease. *Neuropsychology*, *25*(1), 1–14. doi:10.1037/a0020937

Subramaniam, S. R., & Chesselet, M.-F. (2013). Mitochondrial dysfunction and oxidative stress in Parkinson's disease. *Progress in Neurobiology*, *106-107*, 17–32. doi:10.1016/j.pneurobio.2013.04.004

The Huntington's Disease Collaborative Research Group, 1. (1993). A novel gene containing a trinucleotide repeat that is expanded and unstable on Huntington's disease chromosomes. *Cell*, *72*(6), 971–983.

The U S Venezuela Collaborative, Wexler, N. S., Lorimer, J., Porter, J., Gomez, F., Moskowitz, C., et al. (2004). Venezuelan kindreds reveal that genetic and environmental factors modulate Huntington's disease age of onset. *Pnas*, *101*(10), 3498–3503. doi:10.1073/pnas.0308679101

Turek, F. W., Joshu, C., Kohsaka, A., Lin, E., Ivanova, G., McDearmon, E., et al. (2005). Obesity and metabolic syndrome in circadian Clock mutant mice. *Science (New York, N.Y.)*, *308*(5724), 1043–1045. doi:10.1126/science.1108750

van Wamelen, D. J., Aziz, N. A., Anink, J. J., van Steenhoven, R., Angeloni, D., Fraschini, F., et al. (2013). Suprachiasmatic nucleus neuropeptide expression in patients with Huntington's Disease. *Sleep*, *36*(1), 117–125. doi:10.5665/sleep.2314

Vieira, E., Marroquí, L., Batista, T. M., Caballero-Garrido, E., Carneiro, E. M., Boschero, A. C., et al. (2012). The clock gene Rev-erb***α*** regulates pancreatic ***β***-cell function: modulation by leptin and high-fat diet. *Endocrinology*, *153*(2), 592–601. doi:10.1210/en.2011-1595

Vollmers, C., Gill, S., Ditacchio, L., Pulivarthy, S. R., Le, H. D., & Panda, S. (2009). Time of feeding and the intrinsic circadian clock drive rhythms in hepatic gene expression. *Pnas*, *106*(50), 21453–21458. doi:10.1073/pnas.0909591106

Wiegand, M., Möller, A. A., Schreiber, W., Lauer, C., & Krieg, J. C. (1991). Brain morphology and sleep EEG in patients with Huntington's disease. *European Archives of Psychiatry and Clinical Neuroscience*, *240*(3), 148–152.

Wu, L., & Reddy, A. B. (2013). Disrupting rhythms: diet-induced obesity impairs diurnal rhythms in metabolic tissues. *Diabetes*, *62*(6), 1829–1830. doi:10.2337/db13-0353

Youle, R. J., & van der Bliek, A. M. (2012). Mitochondrial fission, fusion, and stress. *Science (New York, N.Y.)*, *337*(6098), 1062–1065. doi:10.1126/science.1219855

Young, K. W., & Greenwood, C. E. (2001). Shift in diurnal feeding patterns in nursing home residents with Alzheimer's disease. *The Journals of Gerontology. Series a, Biological Sciences and Medical Sciences*, *56*(11), M700–6.

Zisberg, A., Gur-Yaish, N., & Shochat, T. (2010). Contribution of routine to sleep quality in community elderly. *Sleep*, *33*(4), 509–514.